Geochemical Attributes of Vaugnerite, Mg-Monzodiorite and Monzonite of Nongpoh - Nongkhlaw Area, Meghalaya; North East India: their tectono magmatic implications.

M.A. Khonglah[1] & Subrato Sarkar[2]

1. Petrology Division, Geological Survey of India, North Eastern Region, Shillong
2. Geological Survey of India, Central Headquarters, Kolkata

Abstract: *Swarm and isolated porphyritic vaugnerite-Mg-diorite dykes spatially and temporally intimate with coarse grained equigranular diorite-granodiorite small plutonic suite and porphyritic monozogranite Nonpoh pluton in the Precambrian Meghalaya-Assam Gneissic Complex of Ri-Bhoi and West Khasi Hills districts, Meghalaya, North East India. Phlogopite/Phlogopitic biotite phenocrysts are set in a hypidiomorphic groundmass of phlogopitic-biotite/biotite, plagioclase, amphibole, ± minor Cpx (diopside), rare Opx, minor K-feldspar and quartz of vaugnerite. The phenocrystic mica and mafic phase drastically decreases in the associated diorite and granodiorite. Accessories are sphene, apatite, magnetite, epidote, monazite, allanite, pyrite and chalcopyrite. Chemically, the vaugnerite corresponds to gabbro, monzogabbro or, monzodiorite rocks; the diorites to gabbroic-diorite and monzodiorite while the granodiorite identifies as monzonite. The vaugnerites are calc-alkaline to tholeiite belonging to the high-K shoshonite series, with abundant compatible elements complementing the moderate to high Mg#, suggestive of an ultramafic source while the diorites and granodiorites are calc-alkaline. MORB normalized elemental plot show enriched LILE (e.g., K, Ba, Th), HFSE (e.g., Zr), LREE (e.g., La, Ce, Sm) and depleted HFSE (e.g., Ta, Nb, Ti & Y) and HREE inferring mixing of mafic/ultramafic magma with granitic magma; with some evidence of melting, assimilation, storage and homogenization (MASH). MORB normalized plot shows a well defined Ta-Nb-Ti (TNT) negative anomaly often diagnostic of calc-alkaline lamprophyres (CAL) that are associated with high K-calc-alkaline rocks in subduction tectonic setting. Abundant rare-earth elements (∑REE ~ 330 to 605 ppm; La_N = 254.85 to 427.27) are similar for the vaugnerite and high Mg-mica-diorite with slight elevation in monzonite samples (∑REE ~ 274 to 749 ppm; La_N = 129 to 427); a manifestation of some assimilation and fractional crystallization (AFC). High REE fractionation trend [$(La/Lu)_{CN}$ = 17 to 22] with high $(Gd/Yb)_{CN}$ ratios (> 2) indicates garnet fractionation that could be linked to a mantle sources that melted at depths of the spinel-garnet [$(Gd/Yb)_{CN}$ > 2] facies for the basic variants. Mineralogy, chemistry of the vaugnerites and high Mg-diorites are comparable to the vaugnerite and durbachite associations of European Variscan orogen of French Central Massif and Corsica of Central Europe that are emplaced in a subduction back arc tectonic setting. The association of these bodies/dykes with the major Pan-African calc-alkaline porphyritic granite plutons (Nongpoh Pluton ~ 520 to 550 Ma) supports the northeastward continuation of the Pryz Bay Suture Zone or collision of India and Antarctica along the Eastern Ghats orogen into Meghalaya-Assam/Shillong Plateau.*

Keywords: Plutonic lamprophyres, gabbro, diorite, porphyritic granite, Precambrian

Introduction: Lamprophyres are a specific group of mafic dyke rocks with mafic hydrous silicates – dark micas and amphiboles – forming phenocrysts while feldspars are confined to the groundmass (Rock, 1991; Woolley et al. 1996; Stemprok, et al, 2014). They are considered to be the product of melting of metasomatized mantle above ancient subduction zones as demonstrated by their high contents of compatible major and trace elements (e.g., MgO, Cr, Ni, mg#) as well as incompatible trace elements (e.g., Cs, Rb and Li). Their high volatile content has often been considered as important in ore forming processes caused or contributed by magmatic fluids (Rock 1991). The association of calc-alkaline lamprophyres with silicic batholiths poses a long-standing problem regarding the genetic relationship between the sources of mafic and felsic magmas. Post-collisional magmatism includes voluminous granitic rocks that were mostly derived by crustal melting (Stemprok, et al, 2014 & references therein). By contrast, subduction of altered oceanic crust, oceanic sediments or continental crust results in metasomatism of the mantle wedge (op. cit) where late-orogenic lamprophyre magmas, in particular calc-alkaline lamprophyre types, form (op. cit). Lamprophyres are usually hypabyssal rocks with occasional volcanic

equivalents and even rarer plutonic equivalents (Rock, 1991). The plutonic equivalents, e.g. appinite, vaugnerite, debauchite, etc, are well documented from the Scottish Caledonian terrain and Central French Massif respectively (Rock, 1991). In Nongpoh area phlogopite/biotite rich plutonic rocks were identified as diorite, granodiorites and more recently as calc alkaline lamprophyric rocks with similar mineralogy to kernsantite (Sarkar, et al, 2007).

The Shillong Plateau regionally exposes Precambrian rocks of Archean to Late-Proterozoic age (Ghosh, et al, 1994; Nandy, 2001; Bidyananda, et al, 2007; Yin, et al; 2010); Permian Lower Gondwana sediments, Early Cretaceous ultramafic-alkaline-carbonatite complex and Sylhet Trap basalts, Cretaceous sediments of Khasi Group, Eocene shelf sediments of Jaintia Group, Oligocene to Pleistocene sediments of Garo Group and Quaternary sediments (Nandy, 2001). Dismembered caught up patches of high grade meta-pelite (sillimanite-corundum rock, khondalite), calc-granulites and two pyroxene basic granulites occur within an undifferentiated Meghalaya-Assam Gneissic Complex (MAGC). The gneissic components constitute an older grey sillimanite cordierite biotite and quartzo-feldspathic para-gneisses emplaced by tonalitic-granodioritic orthogneiss & younger pinkish K-rich granite orthogneiss (Ghosh, 1952; Gogoi, 1975; Khonglah, et al, 2008 & 2010). Patchy metamorphic charnockite are exposed between Kynshi and Nongstoin (Khonglah, et al, 2008 & 2010). The Umsning Schist Belt (USB) unconformably overlies the older gneiss (Devi & Sarma, 2010) but is emplaced by the younger pink granite orthogneiss (Ghosh, 1952a; Khonglah, et al, 2008). The USB and gneissic complex is unconformably overlain by metasediments of the Shillong Group (SG). The 'Khasi Metabasic Intrusives' (Mazumdar, 1976; Hazra, et al, 2015) of hornblende gabbroic composition, at places associate with meta-hornblendite and meta-tonalite/trondhjemite (Khonglah, et al, 2012); are confined within the SG. Several Mid to Late Proterozoic porphyritic granitoid plutons in association with norite/noritic-gabbro - mangerite - quartz-mangerite - charnockite (Khonglah, et al, 2010) and other lamprophyric (similar to kersantite) - diorite differentiates (Sarkar, et al, 2007). Early Cretaceous ultramafic–alkaline–carbonatite complexes intrude both the MAGC and SG (Nandy, 2001). The southern part of the massif is covered by the Sylhet trap basalt volcanics, Cretaceous and Tertiary sedimentary sequences (Nandy, 2001) (Fig-1).

The communication aims at documenting the geochemical attributes of the early vaugnerite and high Mg-mica-diorite differentiates (Sarkar, et al, 2007) of the Late-Proterozoic Nongpoh porphyritic granitoid pluton (Fig-1). These vaugnerite (V) dykes and diorite bodies are intrusive into the MAGC between Korstep in the NE to north of Nongkhlaw in the SW.

Geological Setting of the Study Area: The oldest rock types from the study area comprises Archean to Early Proterozoic metasedimentary supracrustal (khondalite and sillimanite-cordierite metapelite) caught-up-patches/enclaves exposed around Nongdom-Langtor area and Umpyrtha (Gogoi, 1975; Khonglah, et al, 2010). Discrete basic granulite bands occur within the gneisses around Mairang and Jirang. Older cordierite biotite paragneiss occur around Umling, Jirang, Mawrong, and the southern part around Manai and west of Mairang (Khonglah, et al, 2008). The paragneiss coexist along with tonalitic, dioritic to granodioritic orthogneiss around Jirang and Umling. The older para and orthogneiss are henceforth collectively connoted as OG for easier references. The younger pinkish K-feldspar coarse grained rich granitoid orthogneiss (refer to as YG) [Gogoi, 1975, Khonglah, et al, 2008, Khonglah, et al, 2010] dominates the area. The OG forms the basement rocks for the green-schist facies metasediments of Umsning Schist Belt (USB) and Shillong Group (SG) with a basal conglomerate of USB directly and unconformably overlying the OG around Nongkya (Devi & Sarma, 2010). An intrusive relation is depicted between USB and YG (Khonglah, et al, 2008). Variegated schists, quartzites and meta-volcanics define the USB, while two quartzite formations sandwiched a middle phyllite and minor meta-rhyolite/dacite/tuffs formation of the SG. The SG unconformably lies over the USB with a persistent basal polymictic conglomerate (Khonglah, et al, 2008; Devi & Sarma, 2010). The YG constituting sheared and foliated to augen to gneissose syntectonic granitoids are emplaced into the OG, USB and SG. The Khasi Meta-Basics

(refer as KMB) occurring as meta-gabbro/dolerite sills/dykes are restricted to the USB and SG (Fig. 2) [Nandy, 2001; Khonglah, et al, 2008]. Late Proterozoic Porphyritic Granitoid Plutons of Kyllang, Nongpoh and Mylliem emplace the MAGC, USB and SG in the area (Nandy, 2001, Ghosh, et al, 2005, Khonglah, et al, 2008). Mafic rocks of kersantite affiliation to dioritic early differentiates associate with the Nongpoh Pluton (Sarkar, et al, 2007). Small capping inliers of Eocene Tertiary sandstone with minor clay and coal bands occur around Umraleng (near Barapani) and Mairang (Khonglah, et al, 2008).

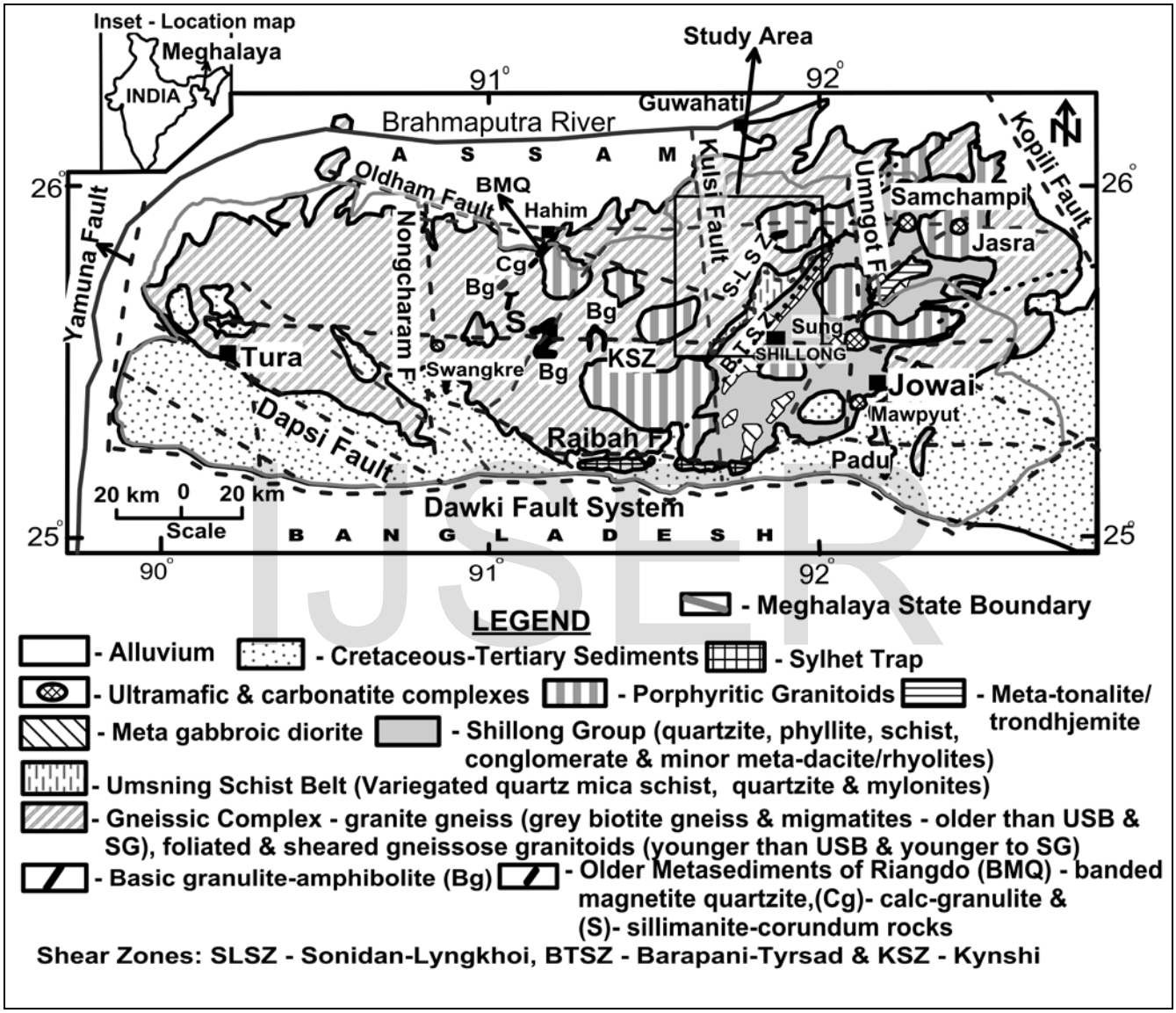

Fig- 1. Regional geological and tectonic framework of the Meghalaya-Assam Plateau
(modified after Mazumdar, 1976, Nandy, 2001, Srivastava, et al, 2004 & Khonglah, et al, 2008)

The gneissosity of the gneisses maintain trends varying from ENE-WSW, NE-SW to occasional NW-SE and in large part is controlled by later porphyritic granitoid emplacements. The contact between the USB and YG is intrusive and subsequently thrusted along NE-SW direction evidenced tight folds with shallow dipping axial planes in SG near to the contact and development of NE-SW to ENE-WSW trending Sonidan-Lyngkhoi Shear Zone (Ghosh, 1952, Bhattcharjee & Rahman, 1985; Khonglah, et al, 2008; Yin, 2010). The USB – YG; porphyritic granitoid plutons-gneiss, Mylliem Granite-SG intrusive contacts are defined by high temperature minerals such as sillimanite, andalusite and cordierite (Mazumdar, 1976, Khonglah, et al, 2008). The Tertiary sandstones display a sub-horizontal to horizontal bedding attitude (Fig-1 & 2).

Field setting and megascopic description of vaugnerite, mica diorites and granodiorite : Small plutonic bodies compositing of diorite, granodiorite and grey granitoids fringes the Nongpoh and Kyllang Plutons that are in turn closely intimated with vaugnerite dykes (Fig-3) of kersantite affiliation (Sarkar, et al, 2007), intrude the gneisses. The biotite rich diorite-granodiorite bodies cover areas between < ½ and 1 sq km; however, around Umling and Umran these occupy ~ 4 and ~ 7 sq km respectively (Fig-2). These coarse to medium grained, homophanous to sub-porphyritic bodies contain enclaves of metasediments e.g. Umran; amphibolite e.g. Umsohphria; quartz patches e.g. Umran & Umsohphria and mafic (vaugnerite) circular enclaves, e.g. Umran and Umling (Fig-4). At Umran the circular quartz patches rimmed by a thin biotite rich layer vary in size from 1 to ~10 cm that forms immiscible blobs of quartz (Fig-5) along with small quartz ocelli. On the other hand the vaugnerite occur as dyke swarm, e.g. Umling & Umran, or, as solitary dykes (Fig-3) within the gneisses preferential to the N-S, NE-SW and ENE-WSW trends. The thicknesses vary from ½ to 75 m with few metres length and an optimum length of ~1 km around Kyrdemkulai. Chilled margins and xenoliths of granitoids are associated with the thicker dykes. Megascopically, vaugnerite are coarse grained, melanocratic to mesocratic and porphyritic with megacrysts/phenocrysts (Fig-5) of phlogopite/phlogopitic-biotite or, biotite set in a medium grained groundmass of gabbroic to dioritic composition (Sarkar, et al, 2007; Khonglah, et al, 2008). Random grain size variation from very coarse to coarse to medium grained, associates with some of the dykes e.g. Kyrdemkulai, Umling, Korstep, Jirang and Nongkhlaw. Usually the medium grained variety flanks the coarse grained centre indicative of chilling effects e.g. Kyrdemkulai and Jirang (for more details see Sarkar, et al, 2007).

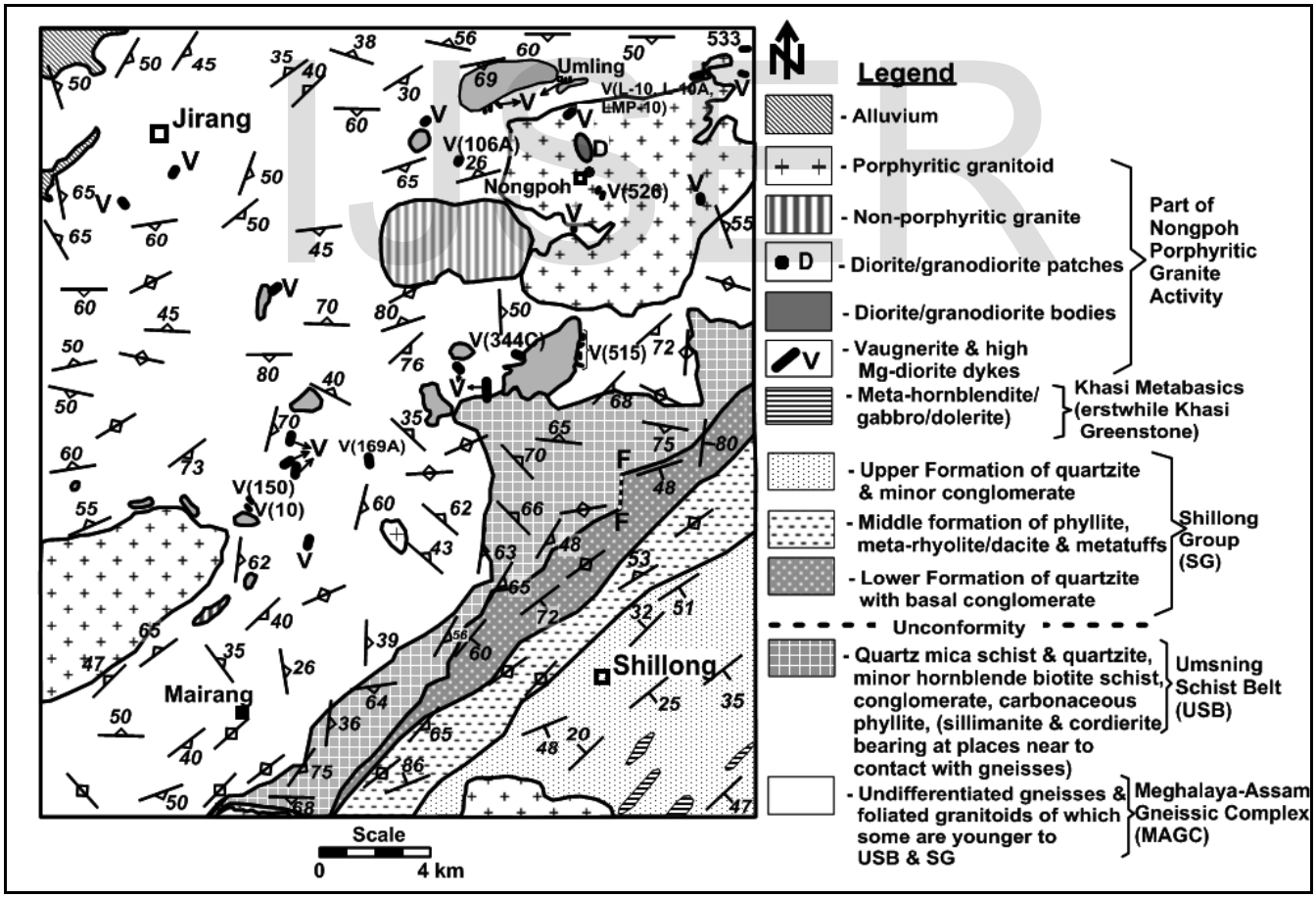

Fig-2. Geological map of part East, West Khasi Hills and Ri Bhoi Districts, Meghalaya (SOI of toposheets 78O/9, 10, 13 & 14)

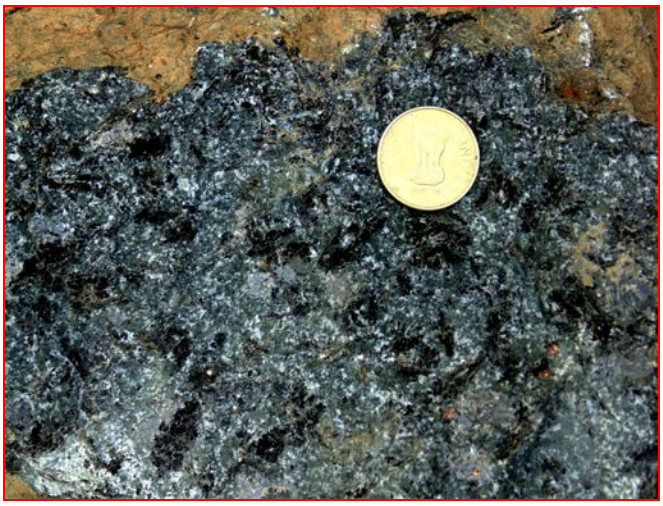

Fig-3. Phlogopitic biotite phenocrysts within medium grained melanocratic amphibole-feldspathic rich groundmass, Stage-III, Power House, Kyrdemkulai. Viewing westerly. Coin- 2 cm.

Fig-4. Partly fragmented vaugnerite-Mg-diorite pillows in granodiorite at Umling, Viewing northerly. Cap lens diameter, 5 cm.

Fig-5. Globular quartz inclusion in coarse granodiorite (monzonite) around Myrdon, Ri Bhoi. Note the biotite crystallization around the inclusion. Coin diameter-2.2 cm

Fig-6. Sharp intrusive contact of Neoproterozoic Nongpoh porphyritic granite & mica diorite around Umta, Ri Bhoi District. Pen - 14 cm

Petrography: The coarse to very coarse grained porphyritic vaugnerite dykes contain phenocryst plates of biotite/phlogopitic-biotite set in a coarse to medium grained groundmass of plagioclase (modal - 23 to 33%, mostly andesine, occasionally labradorite), hornblende (modal - 18 to 30%, mostly magnesio-hornblende, actinolite-hornblende, actinolite), mica (phlogopite or, phlogopitic biotite), Cpx (diopside), K feldspar (modal - 4 to 6%, microcline), quartz (modal - 4 to 8%), myrmekite, apatite, sphene (4% in some samples), zircon, ± opaques (Sarkar, et al, 2007; Roy & Sesha Sai, 2011; present work). The large reddish brown idiomorphic phlogopite/phlogopitic-biotite interlocking phenocrysts with enclose small intergrowths of sphene (Fig-7), plagioclase, Cpx, hornblende, zircon and opaques. Mica occurs in two modes as phenocrysts and as smaller grains in the groundmass. The medium grained hypidiomorphic mica-diorite constitute plagioclase (25 - 30 vol. %), Cpx (diopside-15 - 20 vol. %), hornblende (15 - 20 vol. %), biotite (15 - 25 vol. %), quartz (5-10 vol. %) & K-feldspars (5 - 10 vol. %) [Sarkar, et al, 2007; Roy & Sesha Sai, 2011]. Diopside form intergrowths with both plagioclase and biotite. Primary amphiboles occur as equat intergrowths with pyroxene, quartz, plagioclase and mica (Fig-7A) while, secondary amphiboles are pseudomorphed after pyroxene. Primary platy biotite forms

intergrowth with plagioclase while secondary biotite is pseudomorphed after pyroxene or, amphibole (Fig-7B). Most of the biotite phenocrysts are resorbed particularly along the margin (Fig-7 & 7A) with quartz and K-feldspars while sieve texture is associated with diopside and amphibole (Fig-7B). Both allotriomorphic quartz and K-feldspar are modally more predominant in the diorite variants and have embayed contacts with both plagioclase and biotite but are in sharp contact with both pyroxene and amphibole. Graphic and myrmekite texture is associated with some of the diorite (Fig-7C). Accessories in vaugnerite and diorite mainly consist of elongated to euhedral shaped sphene, apatite, zircon, allanite, monazite and magnetite. Apatite occurs as inclusions in feldspar and phlogopite/phlogopitic-biotite. Big euhedral grains of sphene contain inclusions of opaques and apatite while smaller grains margin the boundaries and cleavage planes of phlogopite/phlogopitic biotite. Opaques are (upto 1 modal %) represented by mainly magnetite, chalcopyrite, pyrite and arsenopyrite.

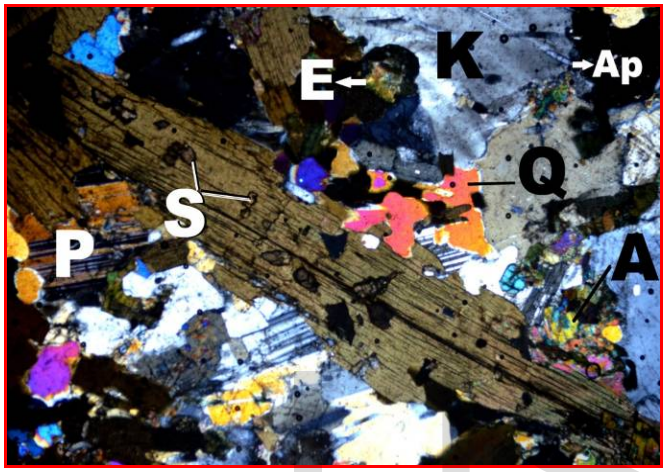

Fig-7. Phlogopitic biotite phenocryst with inclusions of sphene (S) set in groundmass of finer biotite, plagioclase (P), K-feldspar, amphibole (A) & quartz (Q). Ap-apatite, E-epidote. View in cross-nicols (magnification - 4x). Location - Korstep.

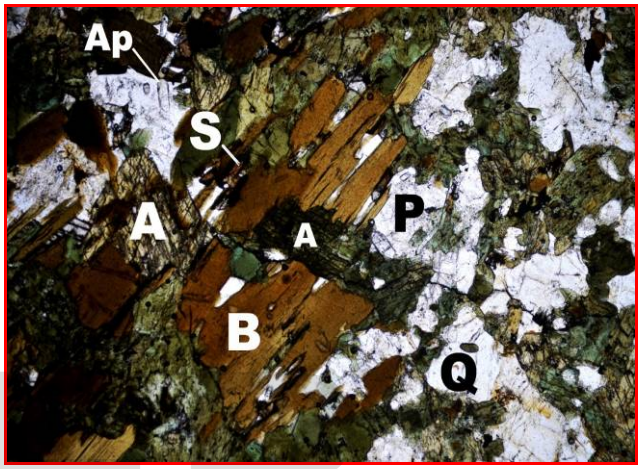

Fig-7A. Partly resorbed phlogopitic biotite phenocryst and hornblende intergrowth with inclusions of sphene (S) set in groundmass of plagioclase (P), amphibole (A) & quartz (Q). Ap-apatite, E-epidote. View in cross-nicols (magnification - 4x). Location - Korstep.

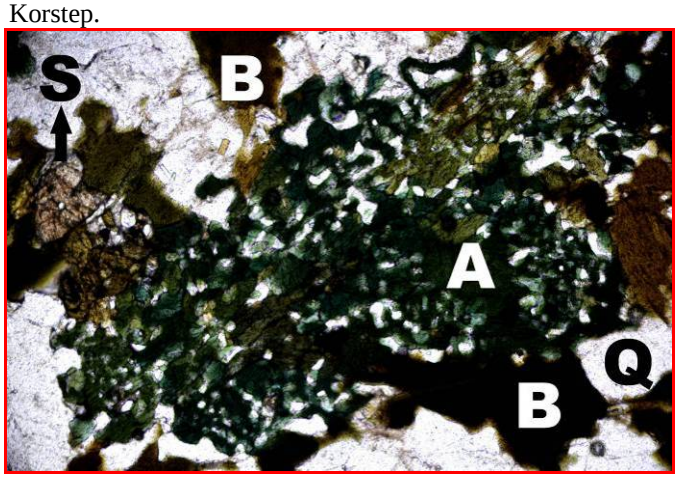

Fig-7B: Sieved amphibole surrounded by altered biotite (B), sphene (S), plagioclase & quartz (Q) in Mg-diorite (magnification - 4x). Location –Umran

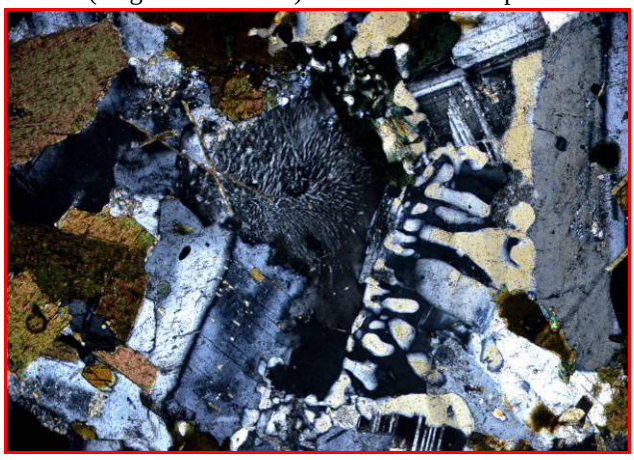

Fig-7C: Graphic & myrmekite reaction texture in Mg-diorite of Umran (magnification - 4x).

Geochemistry:

Methodology: Major oxides and trace-element (Ba, Ga, Sc, V, Th, Pb, Ni, Co, Rb, Sr, Y, Zr, Nb, Cr, Cu and Zn) bulk analysis of representative samples 1, 6, 7 and 9 were analyzed by a fully automated X-ray fluorescence (XRF), PANalytical model MagiX-2424 using end window X-ray tube at the Chemical Division, Geological Survey of India, North Eastern Region, Shillong. The remaining samples were analyzed by Atomic Absorbtion Spectrometry (AAS) method in the Chemical Division; Geological Survey of India, North Eastern Region, Shillong. The REE and other trace elements (Be, Ge, As,Mo, Cd, Sb, Cs, Hf Ta, W and Bi were analyzed by Inductively Coupled Plasma Emission Mass Spectrometer (ICP-MS) in the Chemical Laboratory, Southern Region, Geological Survey of India, Hyderabad, India. The details of techniques, procedure, precision and accuracy of these analyses are described in SOP (http://www.portal.gsi.gov.in/, GSI, 2010). The chemical data of the representative samples are presented in Table-I to III and five more samples of major oxides analysed by Sarkar, et al, (2007) were also considered in the major oxide discrimination plots.

Major oxide geochemistry: As the rocks display wide petrographic and chemical variations, with high MgO and K_2O wt%; both discrimination diagrams used for identification for basic and granitic rocks were used for accurate interpretational purposes. The vaugnerites with SiO_2 - 47.1 to 51.8, MgO- 6.61 to 10.0, CaO-5.06 to 13.64 wt %; are calc-alkaline to tholeiite while the medium grained mica rich gabbroic-diorite bodies with SiO_2-50.9 to 53.4, MgO-8.08 to 16.89, CaO-3.31 to 9.21 wt % are all calc-alkaline (Fig. 8). The high-K shoshonite samples [Table-I, Fig. 8A & B, (Peccerillo & Taylor, 1976)] are mildly enriched in compatible elements e.g. Cr, Ni and V complementing the moderate to high Mg#. Al-[Fe(T)+Ti]+Mg ternary diagram of Jensen (1976) shows komatiitic to high Mg-tholeiite basalt characteristics (Fig-8C) of gabbro, monzogabbro, gabbroic-diorite to monzodiorite compositions (Fig. 8D). In the SiO_2 vs. Na_2O+K_2O binary plot of Middlemost (1985), they are either alkaline to sub-alkaline (tholeiitic) as demonstrated by the Irvine & Baragar, (1971) division line. The associated diorites all straddle in the monzonite field. Normative QAP plot suggest a monzonite composition for most of the samples with a few samples straying into the adjacent fields of diorite/gabbro; monzodiorite/monzogabbro, quartz-gabbro/quartz-diorite and quartz-monzonite (Fig. 8E). The granodiorite classifies in the quartz-monzonite domain (Fig. 8E). Considering their lamprophyric mineralogy (Sarkar, et al, 2007 & present work) the samples were plotted in the $K_2O/(K_2O+Na_2O)x100$ *vs.* $MgO/(MgO+FeOt)x100$ diagram [Rock, 1991] where most samples station in the vaugnerite field, close to the mean compositions of kersantite, minette and vogesite, with a few samples staying close to the basalt and diorite average compositions (Fig. 8F). In the Al_2O_3 vs. MgO binary plot of Buda & Dobosi (2004) the samples featured near to the Massif Central and Corsica vaugnerite domain (Fig. 8G).

All but two samples are potassic, with K_2O/Na_2O ratio in range from 1.12 to 3.87 (Table - I); where the medium grained mica gabbroic-diorite and monzodiorite samples have higher ratios in comparison to the vaugnerite. The variable moderate to very high MgO wt%, Mg# and enriched Cr_2O_3 wt%, or, Cr (ppm) with elevated normative diopside and hypersthene and some samples showing normative olivine indicating a possible ultramafic ancestry. Well defined positive correlation of mg# vs. Cr_2O_3 suggests olivine, pyroxene and spinel fractionation (Fig-8I) for the vaugnerite and high Mg-mica diorites. Strong negative correlation between mg# vs. Al_2O_3 (Fig-8H) infer normal differentiation trend while scattered ill defined trends displayed by mg# vs. SiO_2, Na_2O and K_2O (Fig-8H) invokes hybridization mixing and mingling of a mafic with a granitic magma (Fig-4). This is in accord with occurrence of globular/pillows of vaugnerite, mica-diorite and MME's (present work, Fig-4) earlier inferred as endogenous mafic inclusions (Sarkar, 2007) in granodiorite or, quartz-monzonite; further supported by ill defined trends in Harker's variation diagram (Fig-8I).

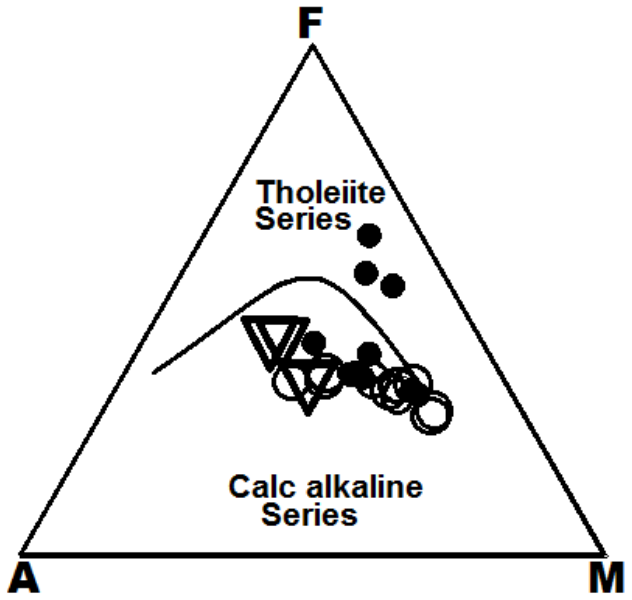

Fig-8: AFM plot of mafic - dioritic rocks. Symbols: Dark circle - coarse grained vaugnerites, Open circles - medium grained mafic to dioritic rocks, Inverted triangle - medium grained monzonite.

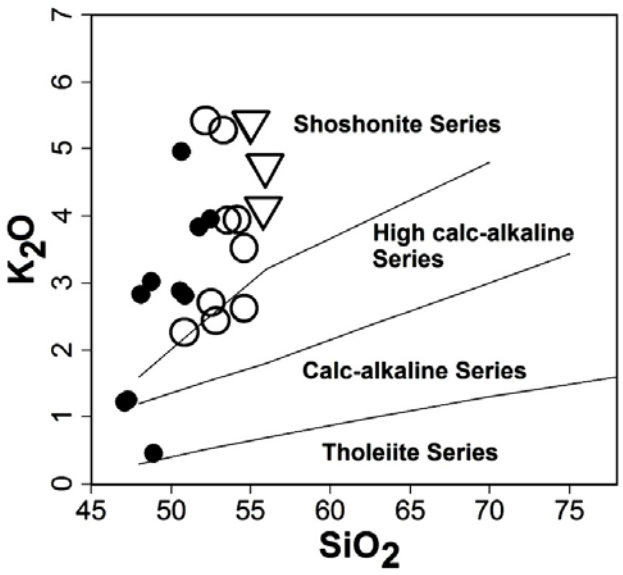

Fig-8 A: K_2O vs. SiO_2 plot after Peccerillo & Taylor, 1976. Symbols same as Fig-8.

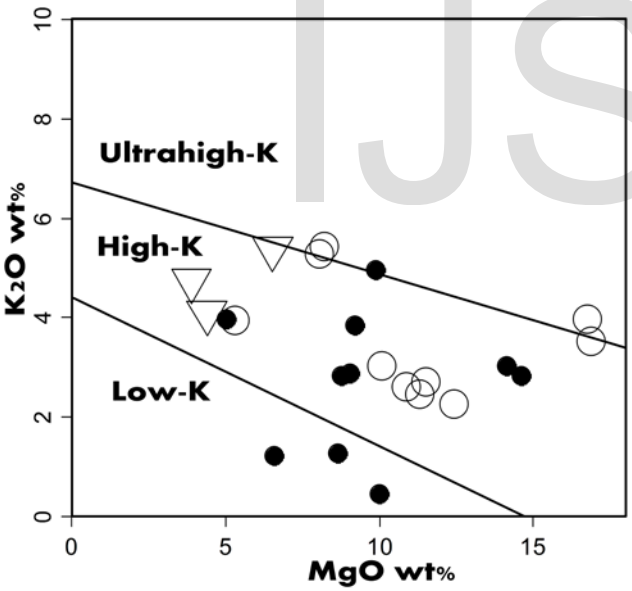

Fig-8B: K_2O vs. SiO_2 plot after Peccerillo & Taylor, 1976. Symbols same as Fig-8.

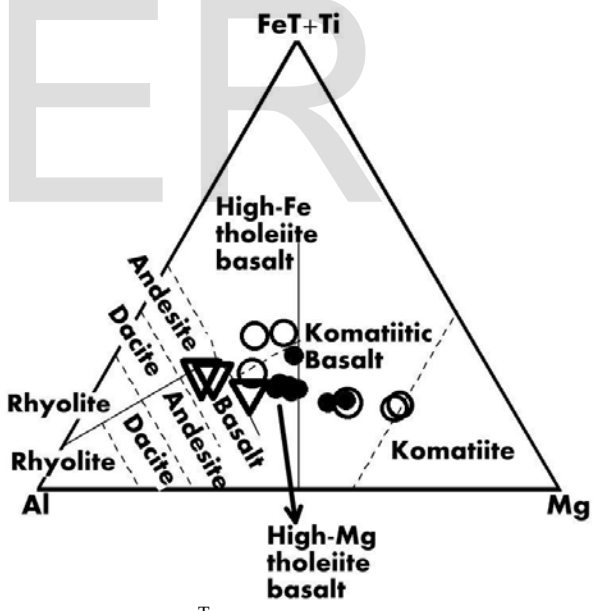

Fig-8 C: Al-(Fe^T+Ti)-Mg ternary plot after Jensen, 1976. Symbols same as Fig-8.

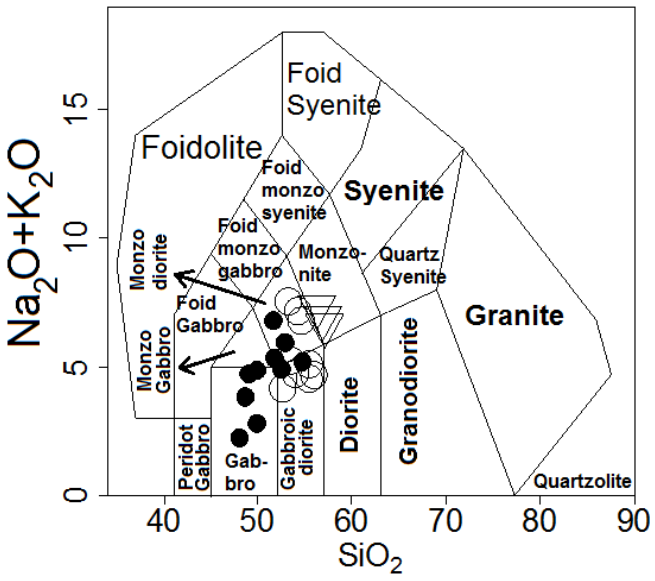

Fig-8 D: TAS plot after Middlemost, 1985. Symbols same as Fig. 3.

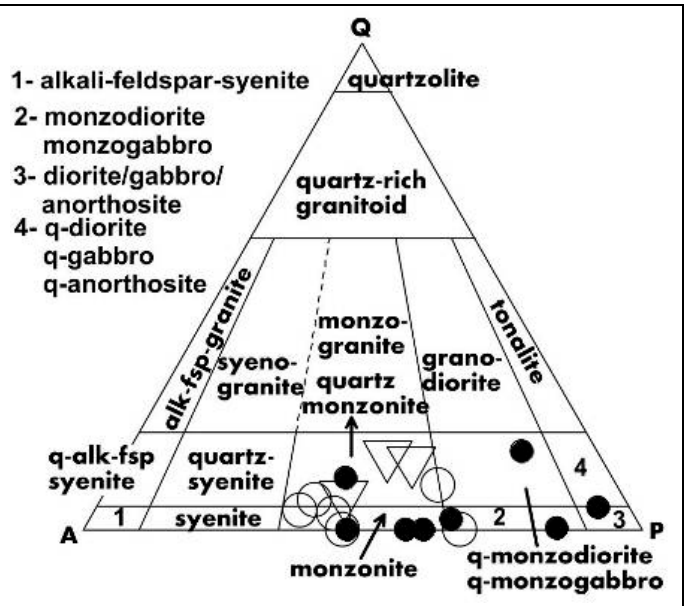

Fig-8E: Norm calculated QAP ternary plot for vaugnerite, diorite & granodiorite of the area. Symbols as in Fig-8.

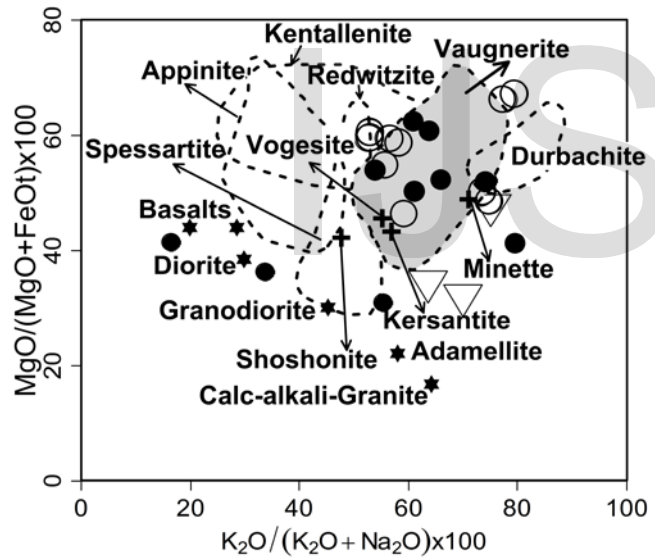

Fig-8F: $K_2O/(K_2O+Na_2O)x100$ vs. $MgO/(MgO+FeOt)$ x100 plot after Rock, 1991. Symbols same as Fig-8. Lamprophyres & their plutonic equivalents (Rock, 1991).

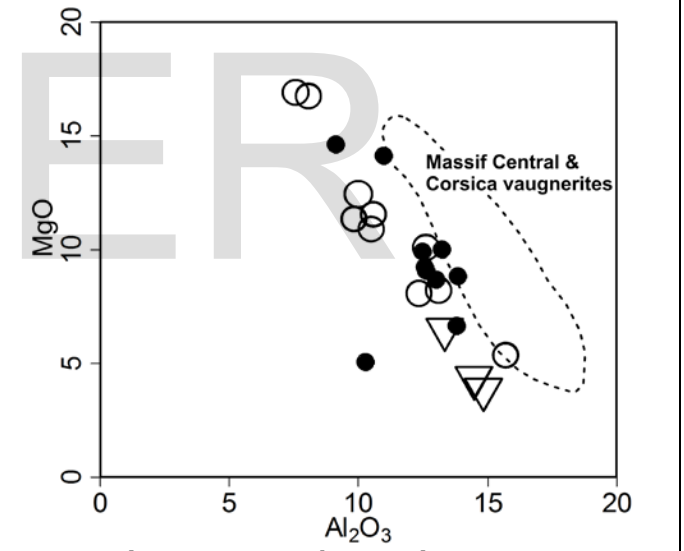

Fig-8G: Al_2O_3 vs. MgO binary plot in comparison to vaugnerite of France (Buda & Gabor, 2004). Symbols same as Fig-8.

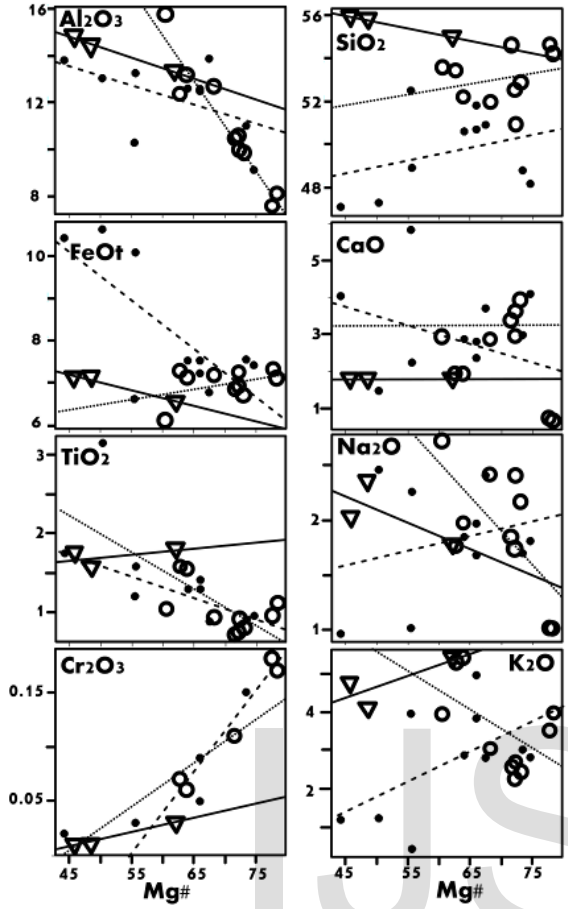

Fig-8H: Mg# vs. other elements variation diagram. Symbols as in Fig-8.

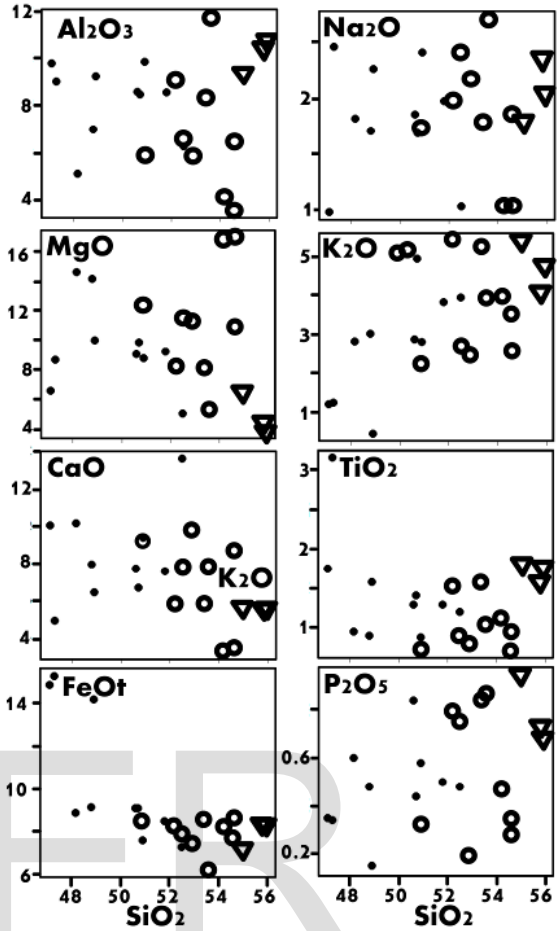

Fig-8I: Harker's variation diagram. Symbols as in Fig-8.

Trace and REE geochemistry: Abundant rare-earth elements of ∑REE ~ 330 to 566 ppm and La_N ~ 209 to 427 in vaugnerite; ∑REE ~ 210 to 605 ppm and La_N ~ 129 to 351 in high Mg-diorites; that slightly are elevated in the monzonite samples (∑REE ~ 274 to 749 ppm; La_N = 179 to 469) manifest some assimilation and fractional crystallization (AFC) (Fig-9). The enriched LREE with respect to depleted HREE typifies normal fractionation trend comparable to shoshonites, K-rich basalts and K-rich mafic - intermediate rocks and lamprophyres (Culler & Graf, 1984) supported by similar Eu/Sm ratio in tune from 0.211 to 0.267. The coarse grained vaugnerite and diorite has fractionation (La/Yb)N ratio in range between 17.00 and 20.04, with one CaO-rich tholeiite dyke indicating least fractionation with no contamination [(La/Yb)N = 45.41]. The ranges are consistent with the group of rocks mentioned above, corroborated by the high REE fractionation trend [$(La/Lu)_{CN}$ = 17 to 22] and considerable depleted HREE as compared to LREE. The smooth negative REE pattern (Nakamura, 1974) with a weak negative Eu anomaly refers to mild plagioclase fractionation (Fig-9) suggesting consanguinity of the variants with different degree of enrichment that is similar for the vaugnerite and diorite and only slightly elevated in monzonite. Sample MORB normalised spider diagram for trace elements (Sun, 1980) of the rocks is consistent with typical average OIB (Fig-10; Winter, 2000) and calc alkaline lamprophyre (CAL) (Fig-10A; Rock, 1991) with a prominent Ta-Nb-Ti negative anomaly characteristic of calc-alkaline lamprophyres (CAL) and calc alkaline rocks evolved in a collisional/subduction tectonic domain . The samples are enriched in K, HFSE (e.g., Th, Zr & Y) and LREE (e.g., La, Ce, Sm) with impoverished HFSE (e.g., Ta, Nb & Ti) and depleted HREE. Trace element and REE discrimination plots based on trace elements after Wood, 1980 (Fig-11) suggest the

samples are derived from a calc-alkaline basalt magma of sub-alkaline to alkaline and andesite composition (Fig-11A) in accordance to the Ta/Yb vs. Th/Yb discriminatory plot of Pearce & Cann, 1983 (Fig.11B) and La/10-Y/15-Nb/8 ternary plot of Cabanis & Lecolle, 1989 (Fig. 11C). The Ta/Yb vs. Ce/Yb and Ta/Yb vs. Th/Yb diagrams of Hastie, et al, 2007, suggest a shoshonitic character (Fig. 11D & 11E) evolved in an active continental margin + alkalic oceanic arcs (Fig-11B). The Ce/Yb vs. Sm variation plot reveals a calc alkaline lamprophyre characteristic for the samples (Fig. 12) while the La/Yb vs. Nb/La variation diagram (Fitton, et al, 1991) infer the samples evolved in the lithospheric mantle near to the average crust compostion (Fig-12A) in an enriched fluid environment (Fig. 12B). The samples were generated from a mantle that is transitional between the garnet and spinel facies melting curves at low degree 3 to 5 % partial melting as indicated by the Ce/Yb vs. Tb/Yb (Fig-12C, Walter, 1998 & Kinzler, 1997) binary plot; that is in agreement with the Sm/Yb vs. Sm diagram which exhibit 1 to 10 % melting of garnet and spinel garnet iherzolite (Fig-12D, Zhao & Zhou, 2007).

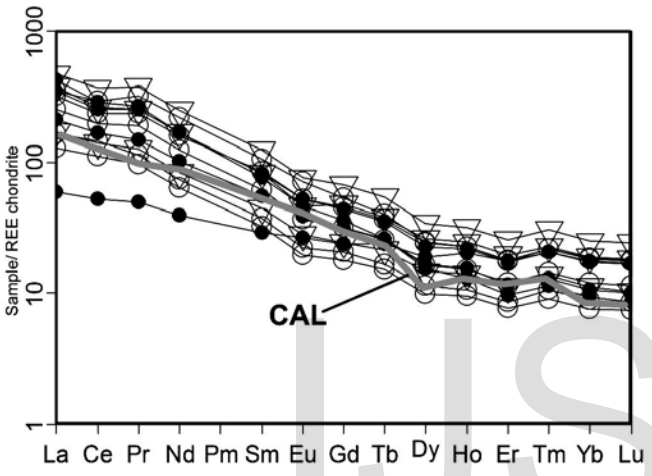

Fig. 9: REE pattern in dyke rocks of the area compared to calc-alkaline lamprophyres. [CAL] (Rock, 1991). Symbols as in Fig. 8.

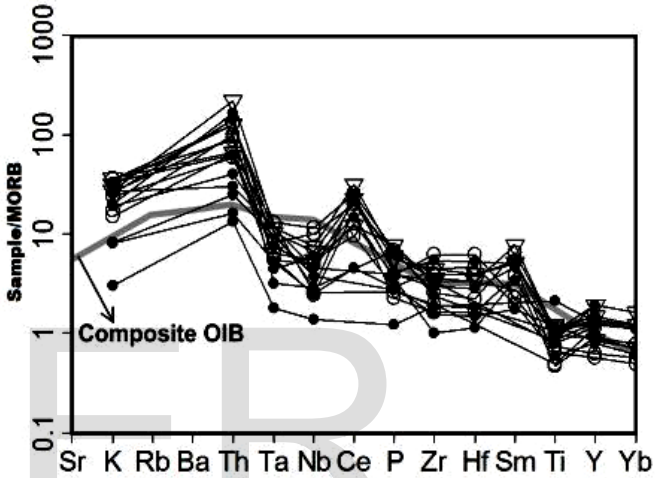

Fig-10: MORB trace spidergram (Pearce, 1983) plot for the samples compared to composite OIB (Sun & McDonough, 1989)

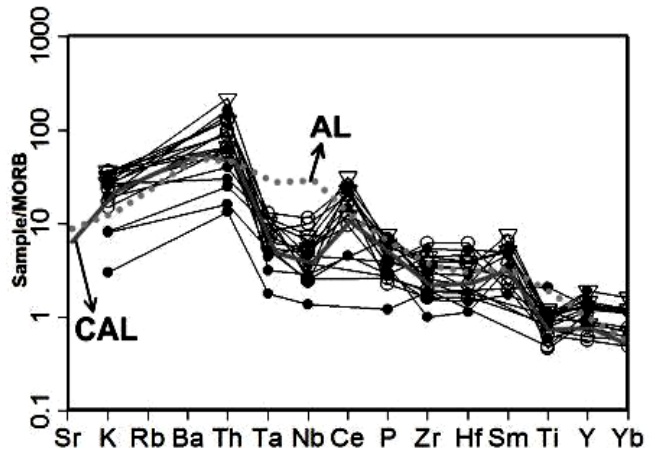

Fig.10A: MORB trace spidergram plot for the samples compared to calc-alkaline lamprophyres (CAL) & alkaline lamprophyres (AL) (Rock, 1991).

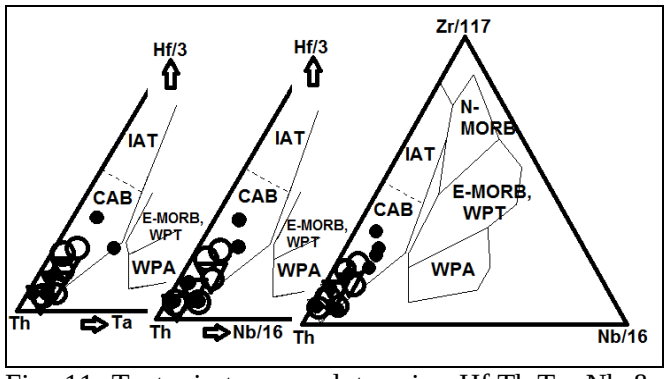

Fig- 11: Tectonic ternary plots using Hf,Th,Ta, Nb & Zr trace elements (Wood, 1980). Symbols same as Fig. 3.

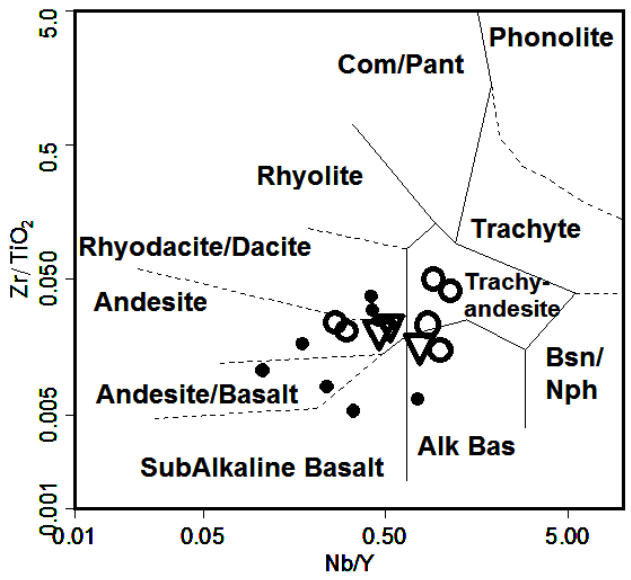

Fig-11A: Zr/TiO2 vs. Nb/Y discriminatory plot (Winchester & Floyd, 1977)

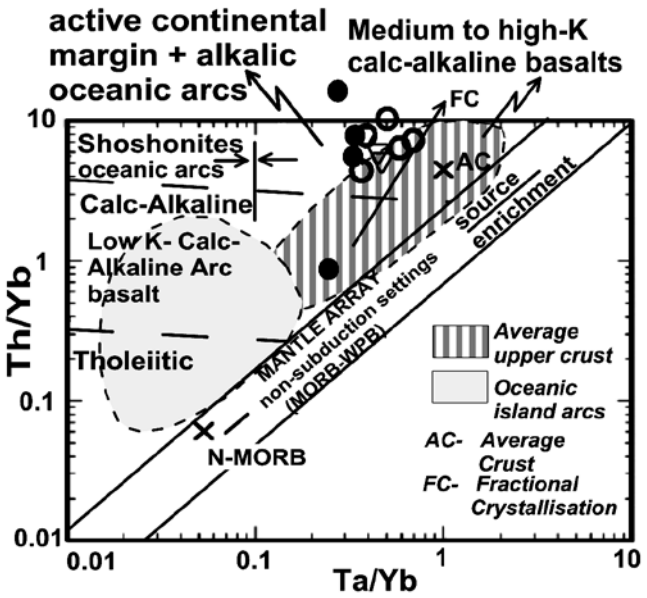

Fig-11B: Th/Yb vs. Ta/Yb tectonic discrimination plot after Pearce, 1983.

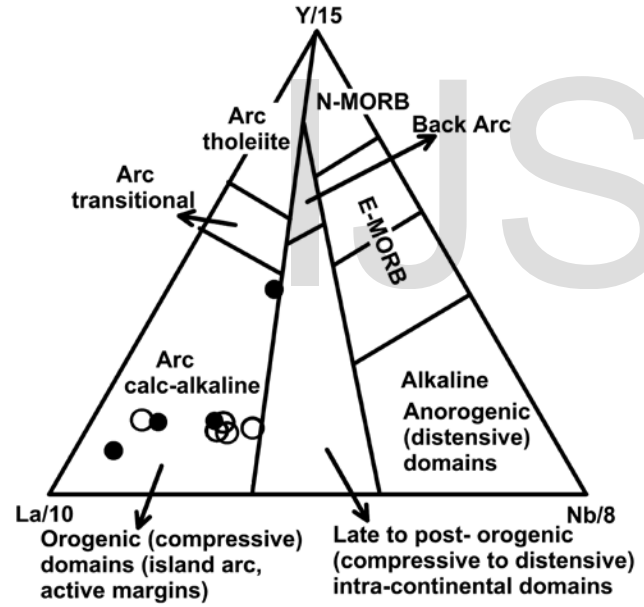

Fig-11C: La/10-Y/15-Nb/8 tectonic ternary plot Cabanis & Lecolle, 1989.

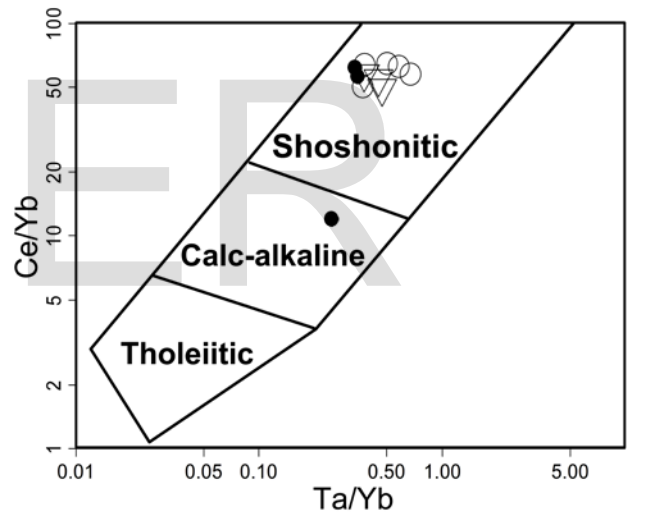

Fig-11D: Ce/Yb vs. Ta/Yb discriminatory plot (Hastie, et al. 2007). Symbols as in Fig-8.

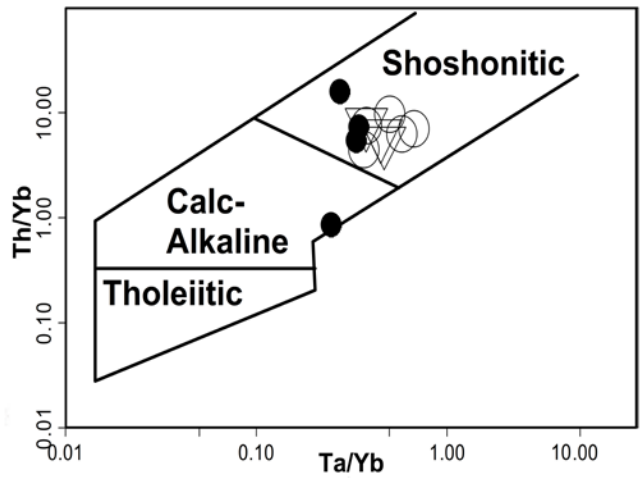

Fig-11E: Th/Yb vs. Ta/Yb discrimination plot (Hastie, et al. 2007). Symbols as in Fig-8.

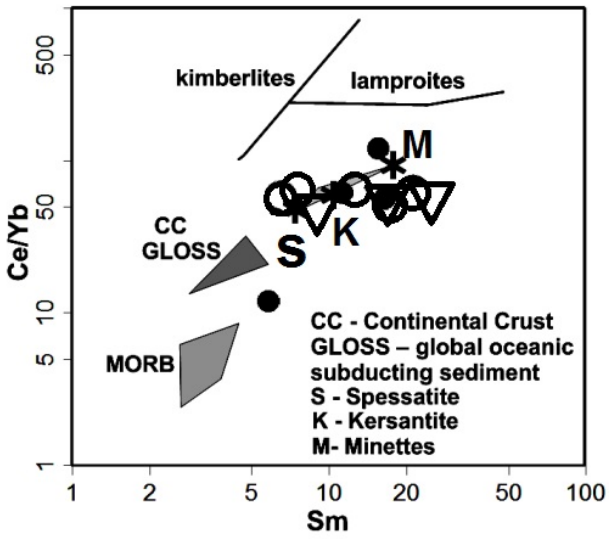

Fig-12: Ce/Yb vs. Sm variation diagram. Symbols as in Fig. 3. (For details see Stemprok, et al, 2014)

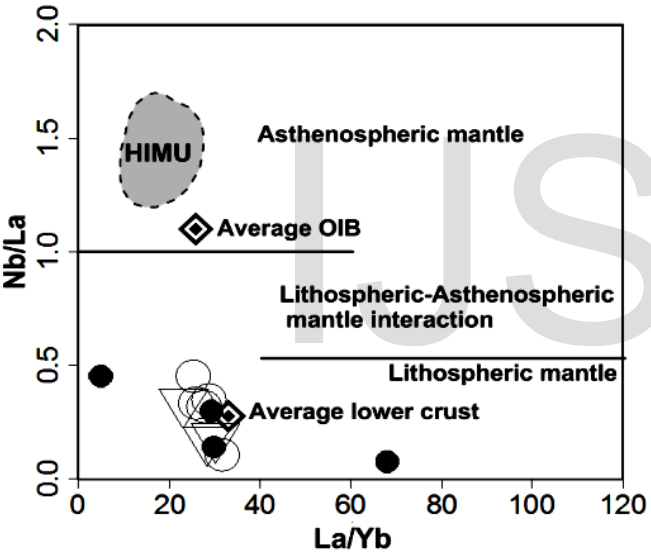

Fig-12A: La/Yb vs. Nb/La variation diagram (Fitton, et al, 1991). Symbols as in Fig-8. [For details see Karsli, et al, 2014].

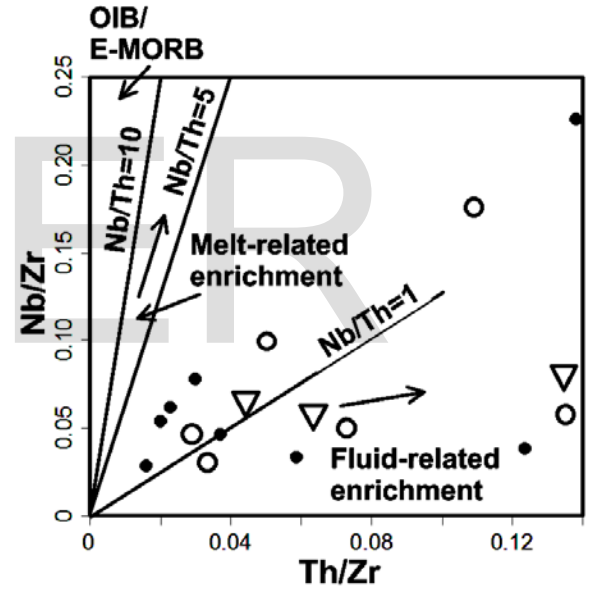

Fig-12B: Nb/Zr vs. Th/Zr binary plot. Symbols as in Fig-8. (Pearce, 2008).

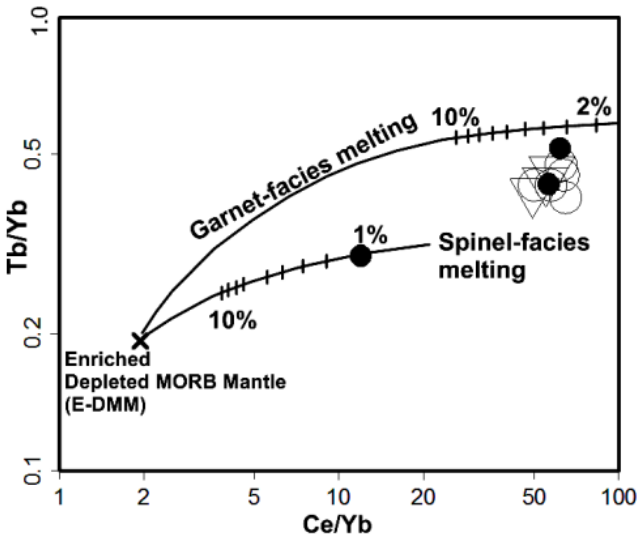

Fig-12C: Partial melting models for the samples. Melting curves after Walter, 1998 & Kinzler, 1997. [For details see Karsli, et al, 2014].

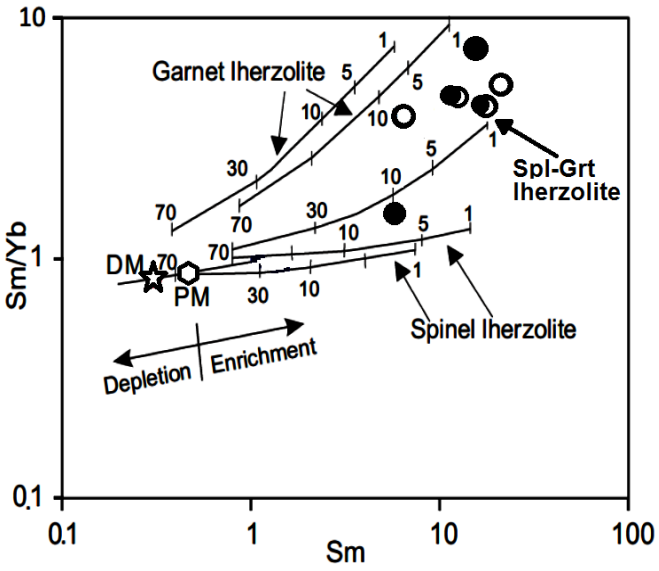

Fig. 12D: Sm/Yb vs. Sm plot (after Zhao and Zhou, 2007) corresponding to 1-10% melting of a transitional mantle between garnet iherzolite and spinel-garnet lherzolite. Melting curves are after Aldanmaz, et al, 2000). DM and PM represents depleted and primitive mantle respectively. A pair of mode and melt mode curves is drawn for spinel (Kinzler, 1997) and garnet (Walter, 1998) lherzolite.

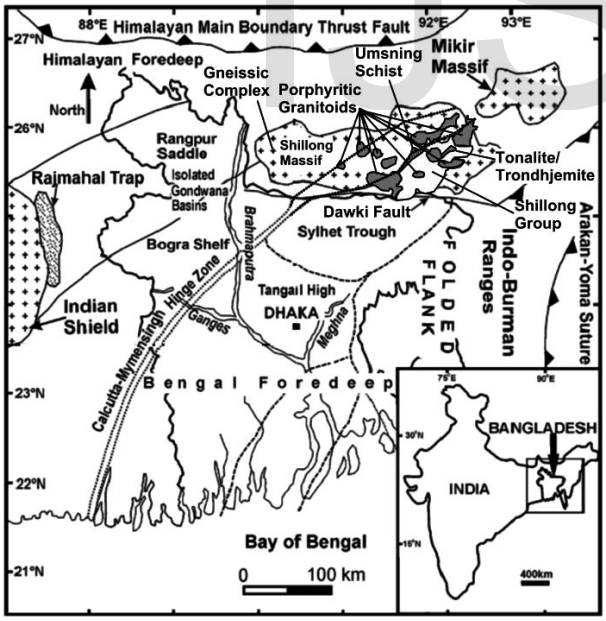

Fig-13: Tectonic map of Bangladesh and Shillong Massif (after Ameen, et al, 2007)

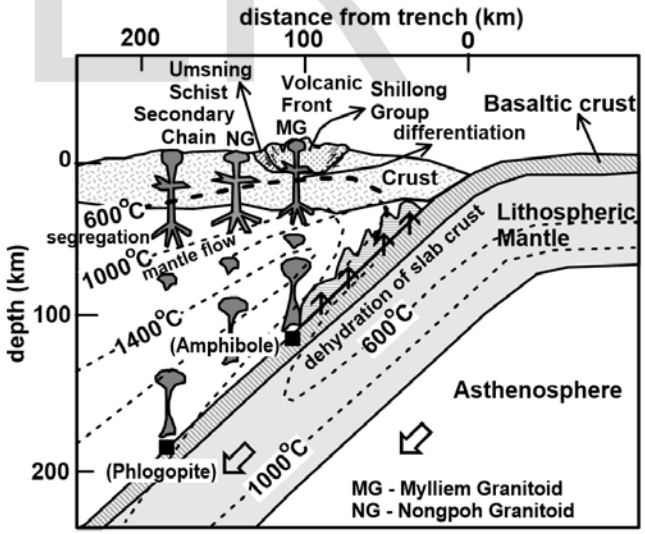

Fig-14: Tectonic collision model of the area possibly during Pan African orogeny (after Winter, 2001).

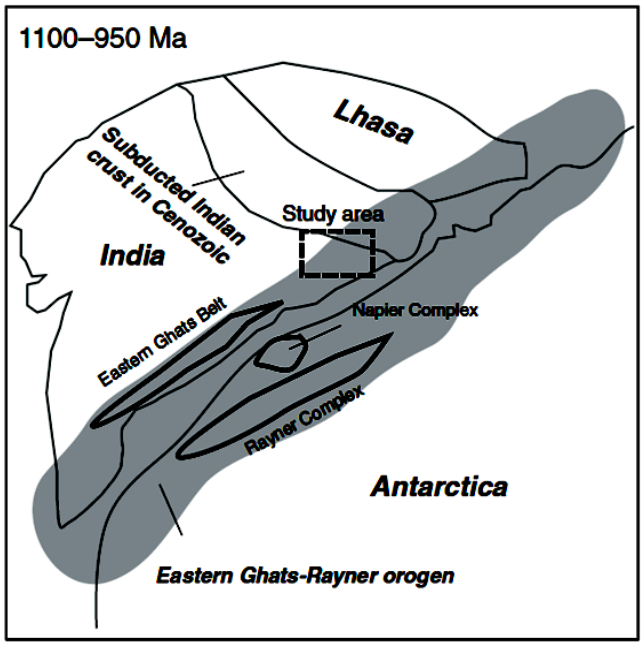

Fig-14A: Tectonic collision model of the area during Grenvillian orogeny (after Yin, et al, 2010).

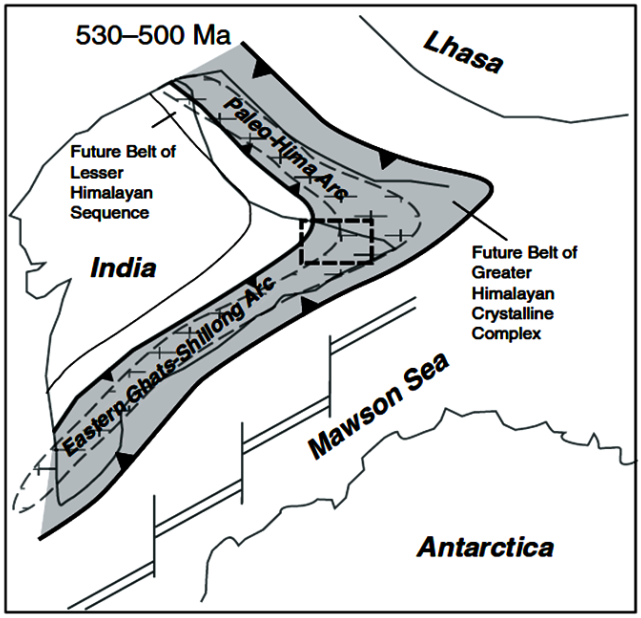

Fig-14B: Tectonic collision model for the area during Pan African orogeny (after Yin, et al, 2010).

Petrogenesis and Tectono-magmatic Setting: Small stocks of diorite-granodiorite plutonic bodies chemically of gabbroic-diorite/monzodiorite and monzonite compositions temporally and spatially associate with vaugnerite dykes, chemically of gabbroic to monzogabbro compositions, around the Nongpoh and Kyllang plutons (Fig-2). Caught up patches of vaugnerite and diorite within the homophanous and porphyritic granitoids (Sarkar, et al, 2007) suggests pre to syn plutonic intrusion. Mica rich diorite association with Mylliem Porphyritic Granitoid near Shillong Peak (Khonglah, et al, 2008) indicate these rocks to be younger than the Mid-Proterozoic Shillong Group metasediments (~1500 Ma) [Rao, et al, 2009]. The Nongpoh Pluton is Rb-Sr dated at ~505 (Ghosh, et al, 1994) Ma while zircon dates reveal an age of ~ 520 Ma (Yin, 2010). Elliptical to globular endogenous mafic inclusions (Sarkar, et al, 2007) identified as vaugnerite and high Mg-diorite in the present work suggest contemporaneous origin of the vaugnerite, Mg-mica-diorite, granodiorite (monzonite) and Nongpoh porphyritic granitoid pluton. Interlocking phenocrystic phlogopite/phlogopitic-biotite in the coarse grain vaugnerite and mica-diorite with abundant inclusions of plagioclase; pyroxene, apatite, and sphene implicate an early crystallisation along with the early phase inclusions that is similar to the mafic megacrystic/phenocrystic phase in calc-alkaline lamprophyres (Rock, 1991) and lamproites (Mitchell & Bergman, 1991). Abundance of phenocrystic phlogopite/phlogopitic-biotite in vaugnerite and some Mg-diorites at places constituting 15 to 30% by volume is comparable with some calc alkaline lamprophyres like minettes and kersantite (Sabatier, 1991; Rock, 1991, Cid, et al, 2002). However, lack of panidiomorphic texture typifying lamprophyres makes classification of these rocks difficult (Sarkar, et al, 2007). Nevertheless, their shoshonitic and lamprophyre characteristics are well constrained by the binary trace element discriminatory plots (Fig-8F, 11B, 11D, 11E & 12). Furthermore, plutonic equivalents of lamprophyres, though still misunderstood, had only recently been well documented (Rock, 1991, Cid, et al, 2002; Couzinie, et al, 2014; Stemprok, et al, 2014, Von Raumer, et al, 2014) for e.g. the appinite suite - diorite association of Scottish, Scandinavian and American Caledonides and the vaugnerite-durbachite series unique for the European Hercynides (op. cit) are the most noteworthy examples. Vaugnerite-durbachite bearing magmas are most likely derived from an enriched mantle source associated with subduction (Von Raumer, 2014 & references therein). Schaltegger (1997) documented the significance of these K–Mg-rich rocks as markers of a suture zone in

the Central Variscan Belt. Broadly, durbachites/vaugnerites though rare, are considered to be granitoid rocks [op. ct] with very sporadic occurrences documented, with the exception of the Variscan fold belt where concentrations are highest. Some monzonitic rocks and high Sr - Ba granites of the Fennoscandian Shield are considered to be equivalent to the Variscan durbachites–vaugnerites [Von Raumer, 2014 & references therein]. Geochemically, the durbachite–vaugnerite rocks show affinities to post-collisional ultrapotassic, mafic to intermediate mantle magmatism of Tibet, North Korea or eastern China [op. ct]. Accepting the common view that magmas of the durbachite–vaugnerite family are extracted from enriched mantle sources require at least, two prerequisites (Von Raumer, 2014). First, these regions, including the Nongpoh-Nongkhlaw of the area under study (present work), must have been underlain by fertile enriched mantle material. Second, a proper tectonothermal trigger must have appeared to get this source melted. The common scenario for building up an enriched mantle reservoir is subduction (op. ct). Aqueous fluids derived from the down going slab infiltrate the mantle wedge and bring along water soluble chemical elements (Fig. 14) [Winter, 2001; Von Raumer, 2014). Where the thermal conditions are appropriate, this fluid input will cause peridotite melting and arc magmatism. Where the melting curve of the peridotite is not overstepped, the mantle will be successively hydrated. The formation of phlogopite in such mantle domains causes an increased fertility with reference to a possible later melting event (op. ct) (Fig. 14). Elements compatible for phlogopite, mainly K, Ba and Rb are strongly enriched in partial melts derived from such a source (op. ct) which is applicable to the vaugnerite, Mg-diorites and monzonite of the study area (Winter, 2001 & present work). Enriched compatible (e.g. MgO & Cr) and incompatible elements (K, Ba, Sr and LREE) invoke generation of hybrid magma (lamprophyric) either through partial melting of a lithospheric mantle or, mixing of basic and felsic magmas or, crustal contamination of a basic/ultrabasic magma. The mica rich mineralogy clearly favours the former, but other factors like fractional crystallisation and crustal contributions may have played their part for the generation of lamprophyric to Mg rich dioritic magmas of the area. These activities are common in subduction zones, where post collisional granitic activity takes place in the later stages during collision relaxation or post collisional collapse (Rock, 1991; Winter, 2001). Similar REE profiles with variable degree of enrichment, of the coarse grained vaugnerite and medium grained Mg-diorites suggest some assimilation and fractional crystallization (AFC & FC) (Fig. 11B, Pearce, 1983) and/or melting, assimilation, storage and homogenization (MASH) [Aldanmaz, et al, 2000] for evolution of these rocks as confirmed by the La/Yb vs. Nb/La binary plot (Fig. 12A) where the samples gathered around the average lower crust of the lithospheric mantle domain while Th/Zr vs. Nb/Zr binary plot (Pearce, 2008) indicate fluid related enrichment of the samples (Fig.12B). Notable enrichment, in increasing order of REE from vaugnerite and Mg-diorite to monzonite reflected the different depth of partial melting of these samples *or*, different rate of crystallisation and differentiation; with vaugnerite dykes tapped from a deeper source. Higher REE enrichment in diorite (monzodiorite) and granodiorite (monzonite) denotes probable derivation from an upper level crustal source. Low Th/La ratio (< 0.3), a sensitive indicator of crustal interaction (Pearce, 1983, Taylor & McLennan, 1985; Sun & McDonough, 1989) suggests significant crustal contribution in this case mixing with granitic melts as evidenced by mixing and mingling features in the field (Fig. 4 & 5). High $(Gd/Yb)_{CN}$ ratios suggest garnet fractionation during formation (>60 km) because the HREE are partially coherent in the garnet phase (Hirschmann, & Stolper, 1996). The mafic dykes with $(Gd/Yb)_{CN}$ > 2 could therefore be linked to mantle sources that melted at depths of the garnet facies invoking presence of garnet as a residual phase in the source except for CaO rich sample with $(Gd/Yb)_{CN}$ of 1.39 of spinel facies (Safonova, et al, 2011) supported by the Ce/Yb vs. Tb/Yb and Sm/Yb vs. Sm plots [Fig-12C, Walter, 1998; Kinzler, 1997] that indicate the samples are derived from low degree partial melt of 1 to 10 % of garnet and garnet-spinel iherzolite mantle (Fig.12D).

In the Meghalaya-Assam Gneissic Complex, porphyritic granitoid plutons overcrowd a zone close to the contact of Gneisses with Umsning Schist Belt along NE-SW and ENE-WSW trends following the Sonidan-Lyngkhoi Shear Zone (SLSZ) [Khonglah, et al, 2008] and the contact of USB with SG along a NE-SW direction

paralleling the Barapani-Tyrsad Shear Zone (BSTZ) [Khonglah, et al, 2008 & 2010, Fig-13] which on a regional scale coincide with the Calcutta-Mymensingh hinge tectonic zone documented from Bangladesh (Ameen, et al, 2007). In MAGC this zone is also affected by charnockitisation and intrusion of norite/noritic-gabbro-mangerite-charnockite suite and associated porphyritic quartz monzonite-monzogranite-granite of South Khasi, Kyllang and Mawdoh plutons (Khonglah, et al, 2010; 2012). Geochronology data suggest a Grenvillian age in range from 1284±60 to 1077±81 M.a. and ~1108 M.a. for the metamorphic and igneous charnockite respectively (Bidyananda & Deomurari, 2007; Bhattacharya, 1986) that coincide with similar dates in younger leucocratic ortho-gneisses (Ghosh, et al, 1994, 2005; Bidyananda & Deomurari, 2007 & Yin, et al, 2010). Conceptualized continent configurations for MAGC involving Antarctica, Australia and India through different periods provided by Yin, et al, (2010) from 1000 Ma; implied that the Pan-African orogeny got overprinted over a Grenvillian belt, which has been postulated for the Eastern Ghat Mobile Belt (Rogers & Santosh 2004) that possibly extends northeast ward into MAGC as first proposed by Crawford, (1974). If these models are presumed be accurate the occurrence of vaugnerite, Mg-mica-diorite in association with monzonite and porphyritic calc-alkaline plutons is profound; because the isotope composition in vaugnerite requires derivation from metasomatically enriched mantle layers about 200 to 800 M.y. old (Bea, et al, 2005) that is accordance to the models put up by Yin, et al, (2010). The abundance of phlogopite or, phlogopitic biotite in the vaugnerite that was derived from melting of a subducted slab below the amphibole facies at depths > 80 km in an back-arc setting (Fig-14, Winter, 2001) that is comparable to the petrogenesis of lamproite and lamproitic rocks (Ayrton, 1991; Cid, et al, 2002; Debon & Lemmet, 1999).

Discussions and conclusions: The Meghalaya Assam Gneissic Complex and adjacent areas of Banglandesh was actively involved in the several breaking and making medley of supercontinents relating to Columbia (Hossain, et al, 2007), Rodinia (Chatterjee, et al, 2007; Bidyananda & Deomurari, 2007) and Gondwana (Crawford, 1974; Ghosh, et al, 2005; Chatterjee, et al, 2007; Bidyananda & Deomurari, 2007). Chatterjee, et al, (2007) proposed the northward continuation of the Pryz Bay suture zone into the Meghalaya-Assam Plateau evidenced by presence of numerous post collisional granitoids in the area (Ghosh, et al, 2005). The Nongpoh pluton dated at ~505 Ma (Ghosh, et al, 2005) or, ~520 Ma (Yin, et al, 2010) is correlated to the Pan-African activity (Crawford, 1974) during assembling of Gondwana supercontinent (Ghosh, et al, 2005). A collision zone had recently been documented from the Shillong Plateau evidenced by bimodal plutonism of Khasi metabasics of meta-hornblendite/hornblende-gabbro composition and meta-tonalite/trondhjemite pluton in Jaintia Hills District (Khonglah, et al, 2012) while the geochemical attributes of the Khasi Metabasics (erstwhile Khasi Greenstone) in Khasi Hills suggested a back arc tectonic setting (Hazra, et al, 2015). The vaugnerite - high Mg-mica-diorite - monzonite and Nongpoh Granitoid association is adding more impetus in support for such a suture/collisional tectonics and possible continuation of the Pryz Bay suture zone into the MAGC (Chatterjee, et al, 2007) or, continuation of the subduction of the Mawson Sea along the east and north sides of India and the development of the Eastern Ghats and paleo-Hima arcs (Yin, et al, 2010) and successive development of the collision of India and Antarctica along the Eastern Ghats orogen and collision between India and Lhasa along the paleo-Hima orogen (Yin, et al, 2010). This association is comparable to the European Variscan orogen of French Central Massif and Corsica of Central Europe; both considered to evolve in subduction zones (Von Raumer, 2014). The first record of the plutonic lamprophyres like vaugnerite, durbachite, amongst others is documented to be associated with monzonite and monozogranite plutons from these zones. Similarly the occurrence of vaugnerite, Mg-mica-diorite in association with monzonite and porphyritic calc-alkaline plutons of the present work, has become critical; because the isotope composition in vaugnerite requires derivation from metasomatically enriched mantle layers about 200 to 800 M.y. old (Bea, et al, 2005) that is agreement to the models put up by Yin, et al, (2010). The abundance of phlogopite or, phlogopitic biotite in the vaugnerite that was derived from melting of a subducted

slab below the amphibole facies at depths > 80 km in an back-arc setting (Fig-14, Winter, 2001) commonly associated with petrogenesis of lamproite and lamproitic rocks (Ayrton, 1991; Cid, et al, 2002; Debon & Lemmet, 1999). However, the authors have only initiated a preliminary study that warrants further advance studies; through futuristic indepth, petrography, mineral chemistry, geochemistry and most importantly isotope and geochronological studies that will unravel a clear understanding of these enigmatic rocks and their role in evolution of the granitoids of the Meghalaya-Assam Plateau and their tectono implications with special reference to Precambrian subduction/collision tectonic setting in the region.

Acknowledgement: *The authors express their gratitude to the Shri. Amarjit Singh; Additional Director General; GSI, NER, Shillong; for his encouragements and permission to publish the data; to Dr. Aparajita Datta, Superintendent Geologist, Petrology Division, Shillong, for the continuous aspiration and support. The support obtained from Officers and Staff-Members of Meghalaya Geology Project, GSI, NER, Shillong is highly regarded.*

References

Aldanmaz, E., Pearce, J.A., Thirlwall, M.F., Mitchell, J.G. (2000): Petrogenesis evolution of late Cenozoic, postcollision volcanism in western Anatolia, Turkey. *J. Volcanol. Geotherm. Res.*, 102: 67-95.

Ameen, S.M. Mahbubul; Wilde, Simon A., Kabir, Md. Zafrul & Akon, Eunuse; Chowdhury Khalil R.; Khan, Md. Sharif Hossain (2007): Paleoproterozoic granitoids in the basement of Bangladesh: A piece of the Indian shield or an exotic fragment of the Gondwana jigsaw?. Gondwana Research 12 (2007) 380–387

Ayrton, S. (1991): The zonation of granitic plutons: the ¨failed ringdyke ¨ hyphotesis: Schweizerische Mineralogische Petrografische Mitteilungen, 68:1-19.

Bea, F.; Montero, P.; Molina, J.F.; Ortega, M.; Scarrow J.H. & Talavera C. (2005): Use and abuse of the term shoshonitic: Shoshonites versus vaugnerites, and minettes. Goldschmidt Conference Abstracts, 2005, Igneous Geochemistry, p - A852.

Bhattcharjee, C. C. & Rahman, S. (1985): Structure and lithostratigraphay of the Shillong Group of rocks of East Khasi Hills of Meghalaya; *Bull. Geol. Min. Met. Soc. India* **53,** 90–99.

Bidyananda, M. & Deomurari, M. P. (2007): Geochronological constraints on the evolution of Meghalaya massif, Northeastern India: An ion microprobe study. Curr. Sci. Vol. 93, pp.1620-1623.

Buda Gyorgy & Dobosi, Gabor (2004): Lamprophyre-derivedhigh-Kmafic enclaves in Variscan granitoids from the Mecsek Mts. (South Hungary). N. Jb. Miner. Abh. Stuttgart, V. 180.2, 115-147.

Cabanis, B. and Lecolle, M., (1989): Le diagramme La/l0-Y/15-Nb/8: un outil pour la discrimination des séries volcaniques et la mise en évidence des processus de mélange et/ou de contamination crustale. Comptes Rendus de l'Academie des Sciences, Paris, series 2, v. 313, p. 2023-2029.

Chatterjee, N., Mazumdar, A.C., Bhattacharya, A., Saikia, R.R. (2007): Mesoproterozoic granulites of the Shillong–Meghalaya Plateau: Evidence of westward continuation of the Prydz Bay Pan-African suture into Northeastern India. Elsevier Precambrian Research, Vol. 152. pp. 1-26.

Cid, Jorge Plá; Lauro Valentim; Stoll Nardi & Pere Enrique Gisbert (2002): Textural Relations of Lamprophyric Mafic Microgranular Enclaves and Petrological Implications for the Genesis of Potassic Syenitic Magmas: the example of Piquiri Syenite, southern Brazil. Pesquisas em Geociências, 29 (2): 21-30.

Couzinie, S., Moyen, J.F., Villaros, A., Paquette, J.L., Scarrow, J.H., Marignac, C. (2014): Temporal relationships between Mg–K mafic magmatism and catastrophic melting of the Variscan crust in the southern part of Velay Complex (Massif Central, France). Journal of Geosciences, 59, 1–18.

Crawford, A. R., (1974): Indo – Antarctic Gondwanaland and pattern of the distortion of a granulite belt. *Tectonophysics*, 22, 141 – 157.

Crawford, A. R. (1969): India, Ceylon and Pakistan: New age data and comparison with Australia; *Nature* 223 80–84.

Culler, R.L. & Graf, J.L. (1984): Rare earth elements in igneous rocks of the continental crust: predominantly basic and ultrabasic rocks. In Rare Earth Element Geochemistry (P. Henderson, ed.). Elsevier, Amsterdam, Netherlands (237-274).

Devi, N.R. & Sarma, K.P. (2010): Strain analysis and stratigraphic status of Nongkhya, Sumer and Mawmaram conglomerates of Shillong basin, Meghalaya, India. Indian Academy of Sciences, *J. Earth Syst. Sci.* 119, No. 2, April 2010, pp. 161–174

Dwivedi, S. B. & Theunuo, K. (2011): Two-pyroxene mafic granulites from Patharkhang, Shillong–Meghalaya Gneissic Complex. Current Science, Vol. 100, No. 1, pp- 100 to 105.

Debon, F., & Lemmet, M., (1999): Evolution of Mg⁄Fe ratios in late Variscan plutonic rocks from the External Crystalline Massifs of the Alps (France, Italy,Switzerland). J. Petrol., 40, 1151–1185.
Fitton, J.G., James, D., Leeman,W.P. (1991): Basic magmatism associated with Late Cenozoic extension in the western United States: compositional variations in space and time. Journal of Geophysical Research 96, 13693–13712.
Ghosh, A.M.N. (1952): On the junction of the Shillong Series and the granite-gneiss on the Mairang-Lyngkhoi Plateau, WSW of Shillong, Khasi Hills, Assam. Rec. GSI, V-82, Pt-2.
Ghosh, S., Chakraborty, S., Paul, D.K., Bhalla, J.K., Bishui, P.K., and Gupta, S.N. (1994): New Rb-Sr isotopic ages and geochemistry of granitoids from Meghalaya and their significance in Middle to Late Proterozoic crustal evolution. Indian Minerals, v. 48, No. 1&2, pp33-44.
Ghosh, S., Fallick, A. E., Paul, D. K. & Potts, P. J. (2005): Geochemistry and origin of Neoproterozoic granitoids of Meghalaya, Northeast India: Implications for linkage with amalgamation of Gondwana supercontinent. *Gondwana Res*., 2005, 8, 1–12.
Hastie, A.R., Kerr, A.C., Pearce, J.A., Mitchell, S.F., (2007): Classification of altered volcanic island arc rocks using immobile trace elements: development of the Th-Co discrimination diagram. Jour. Petrology 48, 2341-2357.
Hazra, Sampa., Ray, Jyotisankar., Manikyamba, C., Saha, Abhishek & Sawant, S. S. (2015): Geochemistry of PGE in mafic rocks of east Khasi Hills, Shillong Plateau, NE India. J. Earth Syst. Sci. 124, No. 2, pp. 459–475
Hirschmann, M.M. & Stolper, E.M. (1996): A possible role for garnet pyroxenite in the origin of the "garnet signature" in MORB. Contrib. Mineral. Petrol. 124, 185–208.
Hossain, Ismail; Tsunogae, Toshiaki; Rajesh, Hariharan M.; Chen, Bin; Arakawa, Yoji (2007): Palaeoproterozoic U–Pb SHRIMP zircon age from basement rocks in Bangladesh: A possible remnant of the Columbia supercontinent. Comptes Rendus Geoscience, 339; 979-986.
Irvine,T.N., & Barager, W.R.A. (1971): A guide to the chemical classification of the common volcanic rocks, Can. Jour. Earth. Sci. Vol. 8.
Jensen, C.S. (1976): A new cation plot for classifying sub-alkalic volcanic rocks. Ontario Div. Mines. Misc. Pap. 66
Karsli, O., Dokuz, A., Kaliwoda, M., Uysal I., Aydin F. (2014): Geochemical fingerprints of Late Triassic calc-alkaline lamprophyres from the Eastern Pontides, NE Turkey: A key to understanding lamprophyre formation in a subduction-related environment. Lithos. 196–197, pp 181–197.
Khonglah, M.A., Khan, M.A., Karim, M.A., Kumar, A., & Choudhury, J. (2008): Geology and structure of the areas in and around Shillong, Meghalaya, North East India, revisited, Proceedings of the National Seminar on Geology & Energy Resources of NE India: Progress & Perspectives Nagaland University Res. Jour. Sp. Pub.
Khonglah, M. A., Imtimkumzuk & Baskaran, R., (2010): Evidence of charnockitisation of granite gneiss around Marwir, Langtor-Nongdom areas WKH, Districts and its implications on the geology of Meghalaya, News, GSI, NER, V. 20 p: 15 - 16.
Khonglah, M.A., Kumar, A. Anil, Mukherjee, P.K. & Haokip, L.T. (2012): Specialised thematic mapping and tectono metamorphic studies of the Gneiss-Quartzite/Schist contact and their stratigraphic relation along the eastern margin of Shillong basin in parts of East Khasi Hills and Jaintia Hills districts, Meghalaya. GSI, NER, Rec. Vol. 144. Part - 4, p-1 -9.
Kinzler, R.J., (1997): Melting of mantle peridotite at pressures approaching the spinel to garnet transition: application to midocean ridge basalt petrogenesis. Journal of Geophysical Research 102, 853–874.
Mazumdar, S.K. (1976): A summary of the Precambrian Geology of the Khasi Hills, Meghalaya, GSI, Misc. Publication No. 23, pt- II, pp: 311-334.
Mazumdar, S.K. (1986). The Precambrian Framework of part of the Khasi Hills Meghalaya, Rec. Geol. Surv. India. V-117(2), pp: 1-59.
Middlemost, E.A.K. (1985): The basalt clan. Earth Sci. Rev., 11, 337-364.
Mitchell, R. H. & Bergman, S. C. (1991): Petrology of Lamproites. New York: Plenum.
Nakamura, N. (1974): Determination of REE, Ba, Fe, Mg, Na and K in carbonaceous and ordinary chondrites. Geochim. Cosmochim. Acta. 38, 757-73.
Nandy, D. R. (2001): Geodynamics of North-Eastern India and the adjoining region. acb-publication, Culcutta.
Pearce, J.A., (1983): Role of the sub-continental lithosphere in magma genesis at acrive continental margins: p. 230-249 in, Hawkesworth, C.J. and Norry, M.J., eds., Continental Basalts and Mantle Xenoliths, Shiva Publishing Ltd., Cambridge, Mass., 272 p.
Pearce, J.A., (2008): Geochemical fingerprinting of oceanic basalts with applications to ophiolite classification and the search for Archean oceanic crust. Lithos 100, 14-48.
Peccerillo, A, & Taylor, S.R. (1976): Geochemistry of Eocene calc-alkaline volcanic rocks from the Kastamonu area, northern Turkey. Contrib. Mineral. Petrol. 58, 63-81.
Rao, J. Mallikharjuna; Rao, G.V.S. Poornachandra; & Sarma, K.P. (2009): Precambrian Mafic Magmatism of Shillong Plateau, Meghalaya and their Evolutionary History. Jour. Geol. Soc. India, Vol.73, 2009, pp.143-152.
Rock, N.M.S. (1991): Lamprophyres. Glasgow: Blackie pub.

Roy, Abhijit & Sesha Sai, V. V. (2011): Final Report on "Petrogenesis of the mafic – ultramafic and dioritic rocks within gneisses in Umling – Lailad – Jirang – Nongkhlaw areas with special reference to its mineral potentiality". Unpub. GSI, Report.

Sabatier, H. (1991): Vaugnerites: Special lamprophyre-derived mafic enclaves in some Hercynian granites from Western and Central Europe. In: Didier, J. & Barbarin, B. (eds.) Enclaves and Granite Petrology. Elsevier, Amsterdam - The Netherlands, pp 63-82.

Safonova, I. Yu., Buslov, M.M., Simonov, V.A., Izokh, A.E., Komiya, T., Kurganskaya, E.V., & Ohno, T. (2011): Geochemistry, petrogenesis and geodynamic origin of basalts from the Katun accretionary complex of Gorny Altai, *(southwestern Siberia)*, Elsevier, Russian Geology and Geophysics 52, 421-442.

Sarkar, S., Khonglah, M.A., Khan, M.A., Kumar, T.B.R. & Ray, J.N. (2007): Polymodal Occurrence of Early Mafic Differentiate Associated with Mid- Proterozoic Calc-Alkaline Plutons of Meghalaya. Journal of Geological Society of India, Vol. 70, July 2007, pp. 53-58.

Sarma K.P. (2014): Shillong Supergroup: A New Lithostratigraphic Unit In The Basement – Cover Precambrian Rocks Of The Shillong Plateau, Northeast India. International Journal of Geology, Earth & Environmental Sciences, Vol. 4 (2); pp. 158-171.

Schaltegger, U., Maurin, J.C., Schulmann, K. and Fanning, M., (1997): U-Pb single grain and SHRIMP zircon dating of granulites and migmatites of the Vosges mountains: multiple melting during rapid exhumation. Terra Nova, 9 Abst. suppl. 1, 112.

Stemprok, M., David D., Holub F.V. (2014): Late Variscan calc-alkaline lamprophyres in the Krupka ore district, Eastern Krušné hory/Erzgebirge: their relationship to Sn–W mineralization. Journal of Geosciences, 59, 41–68.

Srivastava, K, Rajesh, & Sinha, A. K. (2004): Early Cretaceous Sung Valley ultramafic-alkaline- carbonatite complex, Shillong Plateau, North-eastern India: petrological and genetic significance, Mineralogy and Petrology, Springer-Verlag, Austria 80: 241-263.

Sun, S.S., and McDonough, W.F. (Eds.), (1989): Chemical and isotopic systematics of oceanic basalts: implications for mantle composition and processes. Geol. Soc. London Special Pub. U. K. 13-345 pp.

Taylor, S.R. & McLennan, S.M. (1985): *The Continental Crust: Its Composition and Evolution*. Blackwell, Oxford, U.K.

Von Raumer, J. F., Finger, F., Vesel, P., & Stampfli, G.M. (2014): Durbachites–Vaugnerites – a geodynamic marker in the central European Variscan orogen. Terra Nova, 26, 85–95.

Walter, M.J., (1998): Melting of garnet peridotite and the origin of komatiite and depleted lithosphere. Journal of Petrology 39, 29–60.

Winchester, J., & Floyd, P.A. (1977): Geochemical discrimination of different magma series and their differentiation products using immobile elements. *Chem. Geol*., 20: 325- 343.

Winter, J.D. (2001): An introduction to Igneous and Metamorphic Petrology: New Jersey, Prentice Hall.

Wood, D.A. (1980): The application of a Th-Hf-Ta diagram to problems of tetonomagmatic classification and to establish the nature of crustal contamination of basaltic lavas of the British Tertiary volcanic province. Earth Planet. Sci. Lett., 50, pp. 11-30.

Yin, A., Dubey, C.S., Webb, A.A.G., Kelty, T.K., Grove, M., Gehrels & Burgess, W.P. (2010): Geological correlation of the Himalayan orogen and Indian craton: Part1. Structural geology U-Pb zircon geochronology and tectonic evolution of the Shillong Plateau and its neighboring regions in NE India. Geol Soc. America Bulletin. 122; 336-359.

Zhao, J.J., Zhou, M.F. (2007): Geochemistry of Neoproterozoic mafic intrusions in the Panzhihua district (Sichuan Province, SW china): implications for subduction related metasomatism in the upper mantle. Precambrian Research 152, 27-47.

Table-I: Major oxide (in wt %) and CIPW Norm calculations of vaugnerites (1 to 8), Mg-diorites (9 to 14) and monzonite (15 to 17).

Sl No	1	2	3	4	5	6	7	8	9	10	11	12	13	14	15	16	17
Location	**Korstep**	**Umtasor**	**Lower Balian**	**N of Nongkhlaw**	**Umling**	**N of Nongkhlaw**	**Bhalta**	**Byrnihat Power St**	**Korstep**	**Korstep**	**Nongpoh**	**Nongpoh**	**Nongpoh**	**Nongpoh**	**Manipur**	**Nongpoh**	**Umran**
Field remarks	Coarse grained mafic rock (Vaugnerite)								Medium grained biotite diorite						Medium grained biotite granodiorite		
Middle-most, 85	Gabbroic diorite	Monzodiorite		Gabbro		Gabbro diorite	Gabbro		Gabbroic diorite		Monzodiorite		Gabbroic diorite		Monzonite		
SiO2	50.6	51.8	50.7	48.9	48.8	52.5	47.3	47.1	50.9	54.6	52.2	53.4	54.6	54.2	55.9	55	55.8
Al2O3	12.61	12.58	12.5	13.25	11	10.28	13.04	13.8	10.01	10.5	13.13	12.36	7.58	8.1	14.84	13.33	14.43
Fe2O3	3.06	3.79	5.88	5.37	4.53	2.79	4.27	8.71	3.62	3.94	3.58	4.09	2.98	3.32	6.13	2.1	4.21
FeO	6.3	5.04	3.78	9.36	5.04	4.72	11.43	7.02	5.22	4.14	5.04	4.86	5.94	5.22	2.7	5.22	4.5
MnO	0.15	0.14	0.14	0.22	0.15	0.12	0.19	0.26	0.16	0.15	0.14	0.23	0.14	0.12	0.12	0.11	0.14
MgO	9.07	9.23	9.88	10	14.13	5.06	8.68	6.61	12.42	10.87	8.22	8.08	16.89	16.76	3.89	6.53	4.39
CaO	7.75	7.63	6.74	6.48	7.98	13.64	4.97	10.08	9.21	8.75	5.86	5.86	3.48	3.31	5.57	5.6	5.57
Na2O	1.85	1.97	1.68	2.26	1.7	1.02	2.46	0.97	1.73	1.85	1.97	1.77	1.02	1.02	2.03	1.78	2.35
K2O	2.88	3.83	4.95	0.45	3.02	3.95	1.25	1.21	2.25	2.59	5.41	5.27	3.52	3.95	4.74	5.39	4.1
TiO2	1.29	1.29	1.41	1.58	0.9	1.2	3.15	1.75	0.73	0.71	1.53	1.57	0.95	1.11	1.75	1.8	1.57
P2O5	0.84	0.5	0.44	0.15	0.48	0.48	0.34	0.35	0.32	0.28	0.8	0.84	0.35	0.47	0.68	0.94	0.73
Cr2O3	-	0.05	0.09	0.03	0.15	-	-	0.02	-	0.11	0.06	0.07	0.18	0.17	0.01	0.03	0.01
L.O.I.	2.02	1.34	1.06	0.67	1.26	3.29	1.44	1.13	2.51	1.35	1.25	0.77	1.3	1.4	1.08	1.32	1.43
Total	98.42	99.19	99.25	98.72	99.14	99.05	98.52	99.01	99.08	99.84	99.19	99.17	98.93	99.15	99.44	99.15	99.23
K2O/Na2O	1.56	1.94	2.95	0.20	1.78	3.87	0.51	1.25	1.30	1.40	2.75	2.98	3.45	3.87	2.33	3.03	1.74
Norm																	
Q	1.10	-	-	2.26	0.00	5.32	0.18	8.75	-	4.43	-	2.05	2.30	1.63	11.39	4.60	10.23
Or	17.02	22.63	29.25	2.66	17.85	23.34	7.39	7.15	13.30	15.31	31.97	31.14	20.80	23.34	28.01	31.85	24.23
Ab	15.65	16.67	14.22	19.12	14.38	8.63	20.82	8.21	14.64	15.65	16.67	14.98	8.63	8.63	17.18	15.06	19.89
An	17.60	14.17	11.95	24.68	13.46	11.80	20.85	29.73	12.90	12.70	11.00	10.22	5.71	5.86	17.38	12.46	16.72
Di	12.30	16.18	14.49	5.23	18.12	35.84	1.29	14.28	24.32	22.77	10.18	10.58	7.34	5.91	4.52	7.34	4.89
Wo	-	-	-	-	-	3.38	-	-	-	-	-	-	-	-	-	-	-
Hy	23.90	17.70	11.44	32.94	8.84	-	33.60	12.99	21.36	19.82	14.18	18.51	45.74	44.20	7.59	17.83	11.07
Ol	-	1.34	4.53	-	15.69	-	-	-	2.67	-	3.92	-	-	-	-	-	-
Mt	4.44	5.50	8.53	7.79	6.57	4.05	6.19	12.63	5.25	5.71	5.19	5.93	4.32	4.81	4.02	3.04	6.10
Il	2.45	2.45	2.68	3.00	1.71	2.28	5.99	3.33	1.39	1.35	2.91	2.98	1.81	2.11	3.33	3.42	2.98
Hm	-	-	-	-	-	-	-	-	-	-	-	-	-	-	3.36	-	-
Ap	1.99	1.18	1.04	0.36	1.14	1.14	0.81	0.83	0.76	0.66	1.89	1.99	0.83	1.11	1.61	2.23	1.73

Samples – 1, 6, 7 & 9 analysed by XRF and the rest AAS analyses at GSI, NER, Shillong

Table-II: Minor and trace elements analyses of vaugnerite, Mg-diorite and monzonite of the area (in ppm)

Sl No	1	2	3	4	5	6	7	8	9	10	11	12	13	14	15	16	17
Location	Korstep	Umtasor	Lower Balian	N of Nongkhlaw	Umling	N of Nongkhlaw	Bhalta	Byrnihat Power St	Korstep	Korstep	Nongpoh	Nongpoh	Nongpoh	Nongpoh	Manipur	Nongpoh	Umran
Middle-most, 85	Gabbroic diorite	Monzodiorite		Gabbro		Gabbro diorite	Gabbro		Gabbroic diorite		Monzodiorite		Gabbroic diorite		Monzonite		
Ba	2867	na	na	na	na	1261	573	na	1154	na	na	na	na	na	na	na	na
Ga	18	14.6	17.8	19.1	13.6	16	25	19.1	13	12.7	18.1	18.1	12.1	11.9	19.5	17.1	19.1
Sc	24	na	na	na	na	20	25	na	35	na	na	na	na	na	na	na	na
V	240	na	na	na	na	128	650	na	186	na	na	na	na	na	na	na	na
U	<3	3.86	2.33	0.59	4.11	3	<3	0.56	3	5.39	3.31	6.38	1.74	2.16	2.16	1.51	4.78
Th	8	28.3	12.6	2.66	32.9	6	5	3.21	13	19.7	17.7	24.9	11.7	18.7	25.2	13.1	43.7
Pb	30	na	na	na	na	16	13	na	25	na	na	na	na	na	na	na	na
Ni	138	na	na	na	na	408	60	na	177	na	na	na	na	na	na	na	na
Co	39	41.1	30.2	50.4	59.4	65	66	57.6	49	38.4	38.9	31.8	56.9	61.3	23.2	43.9	24.6
Rb	104	na	na	na	na	170	36	na	82	na	na	na	na	na	na	na	na
Sr	1340	na	na	na	na	378	307	na	551	na	na	na	na	na	na	na	na
Y	57	38.7	27.4	45.1	24.1	35	39	36.4	34	27.7	40.5	40.8	16.9	18.8	44.1	25.2	57.2
Zr	215	481	91.2	167	266	299	167	141	178	146	351	228	404	558	397	297	324
Nb	10	16.1	20.6	4.77	10.2	16	13	8.73	9	8.52	34.9	40.1	19.1	17.1	23.1	19.2	26.1
Cr	327	na	na	na	na	807	45	na	708	na	na	na	na	na	na	na	na
Cu	96	na	na	na	na	48	236	na	60	na	na	na	na	na	na	na	na
Zn	96	na	na	na	na	76	128	na	76	na	na	na	na	na	na	na	na
Be	na	2.77	5.02	1.07	3.02	na	na	1.48	na	1.91	4.94	5.61	4.34	4.71	3.92	4.27	3.66
Ge	na	1.37	1.38	1.44	1.28	na	na	1.86	na	1.36	1.52	1.51	1.56	1.62	1.51	1.39	1.61
As	na	<2	<2	<2	<2	na	na	<2	na	<2	<2	<2	<2	<2	7.49	<2	<2
Mo	na	<5	<5	<5	<5	na	na	<5	na	<5	<5	<5	<5	<5	<5	<5	<5
Cd	na	<2	<2	<2	<2	na	na	<2	na	<2	<2	<2	<2	<2	<2	<2	<2
Sb	na	0.92	<0.2	<0.2	0.25	na	na	0.61	na	1.23	<0.2	<0.2	<0.2	<0.2	0.91	<0.2	<0.2
Cs	na	1.68	2.95	0.01	1.24	na	na	3.61	na	1.27	2.42	4.23	2.07	2.02	1.81	3.01	2.67
Hf	na	12.6	2.71	4.41	6.81	na	na	3.58	na	3.86	9.42	5.32	11.1	14.9	9.48	8.09	7.96
Ta	na	1.34	0.79	0.32	0.57	na	na	0.94	na	1.01	1.49	2.34	1.13	0.98	1.85	1.15	2.06
W	na	<5	<5	1.65	7.88	na	na	5	na	<5	4.07	5.71	1.29	2.11	<5	<5	3.79
Bi	na	0.13	0.21	0.1	0.11	na	na	9.02	na	0.12	0.1	0.18	0.1	<0.1	0.1	0.1	0.21

Samples – 1, 6, 7 & 9 analysed by XRF, GSI, NER, Shillong and the rest by ICPMS, GSI, Hyderabad, (na – not analysed).

Table-III: Rare earth element analyses of vaugnerite, Mg-diorite and monzonite of the area (in ppm)

Sl No	1	2	3	4	5	6	7	8	9	10	11	12	13	14	15	16	17
Location	Korstep	Umtasor	Lower Balian	N of Nongkhlaw	Umling	N of Nongkhlaw	Bhalta	Byrnihat Power St	Korstep	Korstep	Nongpoh	Nongpoh	Nongpoh	Nongpoh	Manipur	Nongpoh	Umran
Middle-most, 85	Gabbroic diorite	Monzodiorite		Gabbro		Gabbro diorite	Gabbro		Gabbroic diorite		Monzodiorite		Gabbroic diorite		Monzonite		
La	na	116	69.2	na	141	na	na	19.4	na	84.1	105	116	42.6	54.1	124	56.7	155
Ce	na	217	145	na	249	na	na	45.2	na	169	202	252	96.1	126	225	121	316
Pr	na	28.5	16.4	na	30.1	na	na	5.56	na	21.1	26.4	35.6	10.7	12.7	28.2	14.1	42.1
Nd	na	105	63.4	na	105	na	na	24.6	na	77.5	100	139	39.9	46.6	105	52.1	157
Eu	na	3.99	2.99	na	3.55	na	na	2.03	na	2.81	4.02	5.41	1.51	1.71	3.53	2.14	5.82
Sm	na	16.6	11.2	na	15.5	na	na	5.82	na	12.5	17.3	21.3	6.51	7.55	16.7	8.99	25.1
Tb	na	1.65	1.21	na	1.22	na	na	1.12	na	1.19	1.72	1.89	0.71	0.78	1.79	1.01	2.53
Gd	na	12.1	8.67	na	9.81	na	na	6.51	na	8.71	12.4	14.6	4.94	5.68	13.1	6.72	18.6
Dy	na	7.78	5.65	na	5.29	na	na	6.47	na	5.61	8.28	8.45	3.41	3.87	8.86	4.98	11.7
Ho	na	1.51	1.08	na	0.91	na	na	1.42	na	1.07	1.57	1.57	0.67	0.74	1.71	0.98	2.21
Er	na	3.85	2.59	na	2.17	na	na	3.91	na	2.72	3.96	4.01	1.72	1.94	4.37	2.51	5.76
Tm	na	0.62	0.39	na	0.34	na	na	0.62	na	0.43	0.65	0.65	0.27	0.32	0.68	0.41	0.91
Yb	na	3.86	2.35	na	2.07	na	na	3.78	na	2.65	4.04	4.02	1.67	1.95	4.11	2.45	5.47
Lu	na	0.57	0.34	na	0.29	na	na	0.56	na	0.39	0.61	0.59	0.25	0.29	0.62	0.35	0.82
∑REE	na	519.03	330.47	na	566.25	na	na	127	na	389.78	487.95	605.09	210.96	264.23	537.67	274.44	749.02
Th/La	na	0.24	0.18	na	0.23	na	na	0.17	na	0.23	0.17	0.21	0.27	0.35	0.20	0.23	0.28
Th/Ce	na	0.13	0.09	na	0.13	na	na	0.07	na	0.12	0.09	0.10	0.12	0.15	0.11	0.11	0.14

Samples –analysed by ICPMS, GSI, Hyderabad, (na – not analysed).